AD668966

14 (1)

DEVELOPMENT OF AN ON-LINE IMAGE PROCESSING SYSTEM FOR THE LINC

Technical Report No. 5

February, 1968

Reproduced by the
CLEARINGHOUSE
for Federal Scientific & Technical
Information Springfield Va. 22151

Computer Systems Laboratory

Washington University

St. Louis, Mo.

This document has been approved for public release and sale; its distribution is unlimited.

DDC
RETRIEVED
MAY 16 1968

DISCLAIMER NOTICE

THIS DOCUMENT IS THE BEST QUALITY AVAILABLE.

COPY FURNISHED CONTAINED A SIGNIFICANT NUMBER OF PAGES WHICH DO NOT REPRODUCE LEGIBLY.

DEVELOPMENT OF AN ON-LINE IMAGE PROCESSING SYSTEM FOR THE LINC

John E. Guignon, Jr. and Raymond M. Kline

TECHNICAL REPORT NO. 5

February, 1968

Computer Systems Laboratory
Washington University
St. Louis, Missouri

This research was originally presented to the Electrical Engineering Department of Washington University as a master's thesis by the first author. The work was supported in part by the Advanced Research Projects Agency of the Department of Defense under Contract SD-302 and by the Division of Research Facilities and Resources of the National Institute of Health under Grant FR-00218. Requests to reproduce this document, in whole or in part, should be directed to Computer Systems Laboratory.

"Keep your eyelids up and see what you can see".

Dr. Seuss

ABSTRACT

The development of an on-line image processing system for the LINC (a small digital computer) is described with both hardware and software details being considered.

The purpose of the system is to operate on various types of optical images endeavoring to process them so that a maximum amount of useful information is retrieved for final interpretation by the observer. Besides other processing techniques, contrast enhancement and subtraction have been implemented into the system to achieve this purpose. A mathematical model of the system is investigated and equations describing its capabilities are derived. Results showing several pictures before and after processing as well as data verifying the mathematical model are also presented.

TABLE OF CONTENTS

No.		Page
1.	Introduction	1
	1.1 Main Objective and Scope	2
	1.2 Literature Survey	3
2.	General Description of the Image Processing System	10
	2.1 LINC and Interfacing	12
	2.2 Image Dissector Camera	16
	2.3 Analog Preprocessing Circuitry	24
	2.4 Display Equipment	31
3.	Coordinating Programs	40
	3.1 Scan Program	40
	3.2 Display Methods	48
	3.2.1 Dot Matrix Technique	48
	3.2.2 Intensity Modulation Procedure	54
4.	Contrast Enhancement as a Means of Reclaiming Picture Information	65
	4.1 Description of the Enhancement Process	65
	4.2 Analysis of the Mathematical Model	71
	4.2.1 Introduction	71
	4.2.2 Analysis of Simple Linear System	74
	4.2.3 Analysis of Experimental System	76
	4.3 Experimental Results	87
	4.3.1 Verification of System's Equations with Quantitative Data	88
	4.3.2 Some Typical Processed Pictures	94

TABLE OF CONTENTS
(continued)

No. Page

5. The Subtraction Technique 103

5.1 Some Methods That Have Been Researched...103

5.2 Description of the Present System 105

5.3 Results 111

6. Summary and Conclusion 116

7. Bibliography 120

LIST OF TABLES

No.		Page
1.	Comparison of Present Scanning Devices	23
2.	A Comparison of Experimental and Theoretical Film Densities f Unity Digital Contrast Enhancement	91
3.	A Comparison of Experimental and Theoretical Film Densities for the Digital Contrast Enhancement Shown in Figure 36	91

LIST OF FIGURES

No.		Page
1.	General Block Diagram of System	11
2.	Photographs of the Apparatus	13
3.	Schematic of Internal Operations of Dissector Camera	17
4.	Linearity Test of the Dissector Camera-Preprocessing Circuit Combination	22
5.	Block Diagram of Analog Preprocessing	25
6.	Experimental Comparison of Dissector Camera's Signal with and without Linear Amplification	28
7.	Comparison of Logarithmic and Linear Amplifiers' Density Response	30
8.	Logarithmic Amplifier Response for Various Gains	32
9.	Analog Preprocessing Circuit	33
10.	Dissector Camera's Density Response After Logarithmic Processing	38
11.	Uncorrected Computer Generated Step Wedge	38
12.	Fundamental Flow Chart of a Coordinating Program	41
13.	Flow Chart of Linear Scan Subroutine	42
14.	Example of Processed Image Produced by Horizontal Raster Scan	45
15.	Improved Resolution by Digital Means	45
16.	Experimental Data Representing the Histogram Subroutine's Function	47
17.	Flow Chart for Dot Matrix Display	50
18.	Decision Tree Manifesting the Procedure for Determining the Matrix to be Displayed	52
19.	Example of the Dot Matrix Display Capabilities	53
20.	Flow Chart for Density Wedge Display	55

LIST OF FIGURES
(continued)

No.		Page
21.	Typical Computer Generated Wedge Produced by Modulating the Intensity	56
22.	Experimental and Desired Display Characteristics	58
23.	Transfer Relation Between the Experimental and Desired Display Characteristics	58
24.	Digitally Corrected Display Characteristic	60
25.	Flow Chart for Intensity Modulation Procedure	61
26.	Examples of Positive and Negative Pictures Processed by Intensity Modulation	63
27.	Analog Contrast Enhancement Possibilities	67
28.	Typical Digital Contrast Enhancement Function	67
29.	Flow Chart for Contrast Enhancement Subroutine	69
30.	Mathematical Model of the System	72
31.	Linearity Test of Computer Generated Densities	80
32.	Typical Contrast Enhancement Curves Relating Input and Output Densities to Digital Values	82
33.	Influence of the Contrast Constant, E, and Density Difference on Contrast Gain (for $E \geq 1$)	86
34.	Influence of the Contrast Constant, E, and Density Difference on Contrast Gain (for $E \leq 1$)	86
35.	Plot of Computer Generated Density Wedge	90
36.	Digital Contrast Enhancement Curves	93
37.	Results of Unity Contrast Enhancement	96
38.	Contrast Enhancement Using Film's Complete Density Range . .	97
39.	Contrast Enhancement Proportional to Histogram's Population .	99

LIST OF FIGURES
(continued)

No.		Page
40.	Contrast Enhancement in High Density Areas	100
41.	Contrast Enhancement in Low Density Areas	101
42.	Schematic Illustrating Alignment Procedure	107
43.	Flow Diagram of Vertical and Horizontal Alignment Subroutine	108
44.	Flow Chart for Subtraction Program	110
45.	Input Angiograms for Subtraction	112
46.	Subtracted Image	113
47.	Subtracted Image Showing Misalignment	114

BLANK PAGE

DEVELOPMENT OF AN ON-LINE IMAGE PROCESSING SYSTEM FOR THE LINC

1. INTRODUCTION

In the field of picture processing by computers there is presently a wide variety of work being accomplished. This ranges from computer graphics and machine-aided design (1)* to automatic measurement of the tracks in thousands of bubble and spark chamber photographs (2). The work reported here considers still another aspect of the field and that is the processing of an optical image from a photographic transparency or other source in order to transform the picture information into a form which the observer can more easily use. Thus, the philosophy of the system is to do the job of interpreting optical data by means of a man-computer interactive process. Under supervision of the man the computer performs various linear and nonlinear processes on the original picture in order to accentuate that portion of the information spectrum which is of interest and to attenuate the rest. Once the information is displayed in suitable form, the observer performs the more subtle operations of pattern recognition or other final steps in interpreting the information.

* Numbers in this form are used to indicate references presented in the Bibliography.

1.1 MAIN OBJECTIVE AND SCOPE

In the design and construction of an image processing or pattern recognition system several factors must be carefully considered, namely: (1) cost, (2) reliability, (3) resolution, (4) versatility, (5) on-line capabilities, (6) speed and (7) simplicity. The primary objective of the system discussed here was to research and develop a low cost image processing system that could process many different types and sizes of optical images. The system is electronic in nature and is comprised of an image dissector camera, a small digital computer and an oscilloscope for displaying the processed image. With the small computer, speed and memory capacity are sacrificed in lieu of availability which permits on-line processing. From this the system may be more specifically termed an economical, on-line image processing system for a small computer. The scope of this report is threefold: (1) to describe the design of the system; (2) to explain the computer programs inherent to the operating of the system; and (3) to present the digital and analog procedures for processing images and to discuss the results thus far achieved.

The equipment engaged in the image processing system satisfied most of the above requirements mentioned in the objective. The characteristics and functions of the apparatus, especially those related to the system's performance, were experimentally investigated and verified. The reason for the experiments was to carefully calibrate the major components in order that each might be optimally operated. The procedures and results from the research are presented in this report in conjunction with the equipment's operations.

Several different types of computer programs were designed for operating the image processing system. One such class of programs includes those operations which could not be efficiently or economically accomplished with analog circuits such as scanning the input image and displaying the processed image. With this arrangement the scan and display are not restricted to one specific pattern but may be easily altered through programming.

The problem of poor contrast existing in the optical image is resolved by means of contrast enhancement. This image processing technique, as will be demonstrated, can either be performed with analog or digital methods or both depending on the circumstances. A mathematical analysis of the system's operations on the optical images provides a better understanding of the equipment's capabilities. The resulting equations derived in the analysis are experimentally verified. Another processing method is called subtraction which as the name implies subtracts two optical images from each other and displays a difference image. The process is implemented by a computer program exemplifying the image processing system's capabilities to scan in any desired manner. The subtraction technique has been applied to a typical problem with reasonable success as is illustrated later. The procedure and quantitative results of these processing methods are described and thoroughly explained.

1.2 LITERATURE SURVEY

A survey of the literature relating to the field of image processing was conducted. The subjects that were considered concerned other current operating image processing systems, display and scanning equipment, physical and psychological properties of images and possible

future applications for image processing systems. The results from the survey have been considerably condensed and are presented in this section.

One of the more successful image processing systems which has been developed is that by Nathan (3) at the Jet Propulsion Laboratory in Pasadena, California. Nathan considers the detailed operations and analyses that have been used for processing pictorial information, especially vidicon television pictures, transmitted by spacecrafts. He described some of the digital procedures for reducing such problems as geometric distortion, random noise, scan-line noise and the limited bandwidth of the system. The geometric distortion of an image is corrected by means of a calibration grid which is exposed under the same conditions as the actual picture. The random noise which results from a poor signal to noise ratio is removed by replacing bad data with the average of neighboring points. Scan-line noise is generated by the nonuniform response of the television camera with respect to successive scans. A two dimensional scan-line noise filter was devised by Nathan to minimize such noise. The filter involved averaging the neighboring scene's brightness and comparing it against the average of the scan line. The difference between the scene average and the line average is then applied as a correction to the point being processed. If the dimensions of important objects in the image are smaller than the scan beam, there is a significant loss in the transmitted resolution; in other words, the higher frequencies become severely attenuated. A one dimensional frequency recovery Fourier filter was designed based on the reciprocal frequency response curve of the system. The results obtained after applying these digital processing techniques were significantly

improved with better resolution and more usable information. However, one of the limitations of Nathan's system is that it does not have on-line capabilities. In other words, the entire picture must be recorded on magnetic tape before any processing can occur. Furthermore, the Jet Propulsion Laboratory work does not appear to make much use of contrast enhancement, a process considered in this report.

Selzer (4) has slightly modified Nathan's system to process radiographs for better human interpretation. Two digital methods that Selzer discusses are frequency-response enhancement of roentgenograms and subtraction of two time related radiographs. The former procedure is based upon a digital filter whose transfer function is the reciprocal of the modulation transfer functions of the roentgen system (5,6). Examples of filtered pictures are presented showing an overall general sharpening of the images. The subtraction technique endeavors to emphasize the difference between two radiographs. The process involved correcting for geometric distortion and then subtracting the two pictures point by point and displaying the absolute difference. Some quantitative results that were obtained by applying the subtraction method to various types of radiographs are exhibited. One good example presented is the subtraction of two chest radiographs taken six months apart. To minimize for exposure and development differences, the above digital high pass filter was applied to the input radiographs. The subtracted image does indeed point out an abnormal condition; however, it is possible that it would be detected by an experienced radiologist in the unprocessed picture. Although the results are encouraging, the system is not on-line as mentioned above and in order to produce satisfactory results, the time interval between initial data and final picture may

approach days. For the on-line image processing system discussed in this report, a subtraction procedure has been designed and is described in Chapter 5. Some of the other subtraction techniques that have been investigated and described in the literature are also compared in that chapter.

The scanner of an image processing system is a device employed to convert optical images into electrical signals. The quality of an image processing system largely depends on the quality of the scanner; therefore, the features of the various devices must be carefully considered in the perspective of the problems to be undertaken. Currently, flying-spot scanners and television cameras are the most widely used electronic scanners. Fink (7) has described the basic optical to electrical conversion principles and operations of these two types of scanners. Fink also discusses some of the attractive features that make one particular device more applicable to a particular situation. For example, flying-spot scanners are practical for high resolution work and are fairly fast. On the other hand, television cameras have high scanning speeds but only moderate resolution. Some of the other features of these devices are presented in Section 2.2.

The resolution of the scanner is an important feature that must be examined when setting up a system. Brown (8) has classified the factors which influence the resolution of flying-spot scanners into four categories, namely: (1) cathode-ray-tube spot size, (2) lens resolution, (3) phototube signal to noise ratio, (4) film image contrast and sharpness. The cathode-ray-tube spot size is primarily a function of beam current whereby the spot size increases with current. Lens resolution may degrade the resolution of the system in three ways:

diffraction effects, aberration effects and light gathering capability. The diffraction and aberration effects are opposing factors in that at maximum aperture, diffraction is a minimum and aberrations are normally large. The opposite holds true for the minimum aperture. As for light gathering, less light is gathered as the lens moves further away from the tube. This implies that light gathering is a function of reduction or magnification. The signal to noise ratio of the cathode-ray-tube decreases when large optical images are reduced for scanning, when a small lens aperture is used or if the cathode-ray-tube spot size is small. Experimental results presented by Brown verified the above expectations. Thus, high resolution is attainable only after all these factors are optimally adjusted and since several are interactive, this involves a trial and error procedure.

A multiple image sensing device, called a Di-Scan which is based on the image dissector principle, is described by Nielsen and Ford (9). The significant aspect of the Di-Scan is that three scanning apertures are available; hence, each provides an individual indication of image density. This device has been particularly instrumental in contour tracing but it does not appear to contribute significantly to contrast enhancement, subtraction of pictures or in any of the other areas of interest to this report.

Another integral part of an image processing system is the display apparatus whereby digital information is transformed into visual information. A comparison and discussion of several different display technologies are presented by Hobbs (10) and Van Dam (11) with particular emphasis on computer displays with only two levels. Some of the more

important characteristics that are discussed in these references are brightness, contrast, reliability, response time, generation rate and storage. Quantitative measurements of these parameters are some of the major problems in the display field. The cathode-ray-tube presently dominates the field for console displays but other display techniques involving lasers, optic-magnetics and electroluminescence are being researched.

In the image processing systems of interest to this report, the human observer is the ultimate user of the information; hence, the properties of human vision must be considered in the deisgn of the system. A series of papers (12,13,14) has recently appeared evaluating redundancy reduction in television pictures; these articles consider parallel problems related to the interest of this report. For example, Schreiber discusses the problem of false contours which may be produced in an area where the subject had no detail if too few shades of gray are allowed by the system. Some of his conclusions are: (1) that almost all pictures will require somewhere between 16 and 256 levels of gray; (2) that quantization noise is more visible than additive random noise of the same r.m.s. value; (3) that outlines are extremely important in perception; and (4) that noise is more visible in blank fields than superimposed on pictures. Experiences during this research tend to verify the above conclusions.

One example of where an image processing system might be applied is to the preprocessing of pictorial data for photointerpretation, which is discussed by Holmes (15). The procedure involves automatically locating targets on a photograph and then classifying them according to some predetermined pattern recognition processes. To facilitate the

classification problem, nonlinear, two dimensional filters were implemented by the program which preprocesses the image. The filtering produced useful results when applied to a specific situation. Holmes also states that scanning and storing the entire image before processing could be averted if an on-line scanning device is used. The scan pattern, of course, would be controlled by the computer; hence, the photograph serves as a read only random access memory.

Solomonoff (16) and Minsky (17) have thoroughly described the progress of artificial intelligence to date. The object of the field is to devise machines to perform various operations that normally require human intelligence. To closely simulate human intelligence, the final artificial intelligence systems should have eyes since human eyes do much information processing. Therefore, an image processing system which could translate the visual data into digital information and perform processing techniques would be of great assistance in resolving some of the artificial intelligence problems. For other possible future applications of an image processing system see references (18,19).

2. GENERAL DESCRIPTION OF THE IMAGE PROCESSING SYSTEM

In assembling this image processing system, the apparatus was kept as simple as possible consistent with good performance. The present arrangement consists basically of the following: (1) the LINC (Laboratory Instrument Computer); (2) image dissector camera; (3) input preprocessing circuitry; and (4) auxiliary oscilloscope for the output display. Each of these elements will be evaluated in this chapter emphasizing those particular characteristics that pertain to the system's operation.

A simplified block diagram describing the overall system is presented in Figure 1. All functions are serially executed with the LINC as the system's coordinator. Briefly, the light source illuminates a transparency for viewing by a photosensitive device, the image dissector tube, which sequentially transforms specific density points of the optical image into proportional electrical signals. This signal is then analog preprocessed and converted to a digital number for processing by the LINC. After this, the computer transmits an analog voltage signal to the output display where a point is intensified on the auxiliary oscilloscope in proportion to the voltage. Each point in the input image is cycled through this procedure one point at a time. For an output display with multilevels of gray, the output image is normally recorded on fast development film with a camera. Because of the length of time, two to four minutes, involved in processing a 500 by 500 point input image, a time exposure is essential. The entire operation is referred to as on-line scanning since the output display is available for analysis in a matter of minutes after the initialization of the scan.

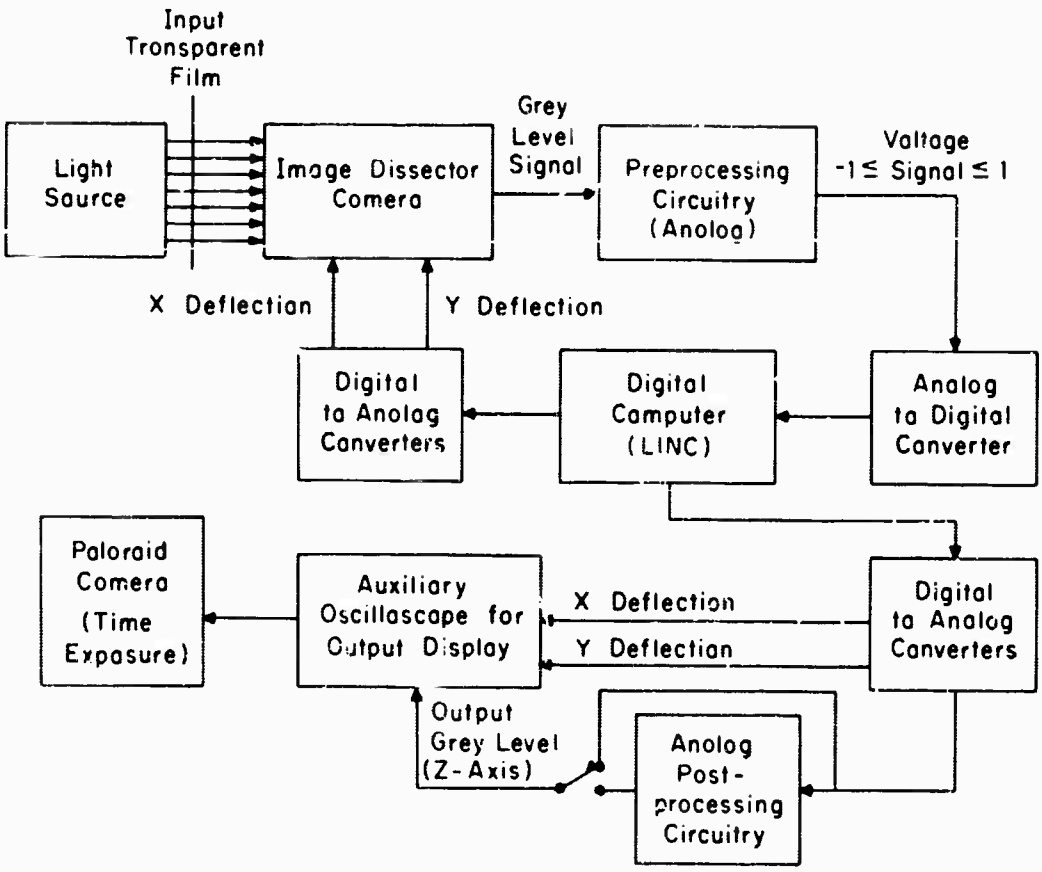

Figure 1. General Block Diagram of System

Figure 2 shows pictures of the apparatus engaged in this image processing system. As the pictures reveal, each component is mobile; moreover, the scanning and display equipment occupy a small amount of space as compared to the LINC.

2.1 LINC AND INTERFACING

The LINC (20) will be described first because of its central position to the overall functioning of the system as illustrated in Figure 1. Several different operations are executed by this computer during a scan, namely: (1) driving the horizontal and vertical scan; (2) sampling an analog voltage signal; (3) processing the sampled voltage; and (4) displaying an output image. Only the hardware characteristics of the LINC pertinent to operating the system will be explained.

The LINC is a small and comparatively inexpensive digital computer which was specially designed to aid the human researcher in perpetrating various on-line experiments. It has a twelve bit word length with 2048 internal memory locations and an additional storage capacity of 131,072 words on magnetic tape. However, the tape storing and retrieving times are on the order of seconds and are usually avoided whenever possible. The average time for the execution of one LINC instruction is approximately sixteen microseconds.

In the earlier stages of the image processing system, a computer program was written utilizing the magnetic tape for storing the complete input image. With the input on tape various digital functions could process the image endeavoring to improve the quality of the output image. However, the extra time for storing and retrieving information on tape is much greater than the time required to reliably rescan the input image with a different digital or analog process. Because of the rather

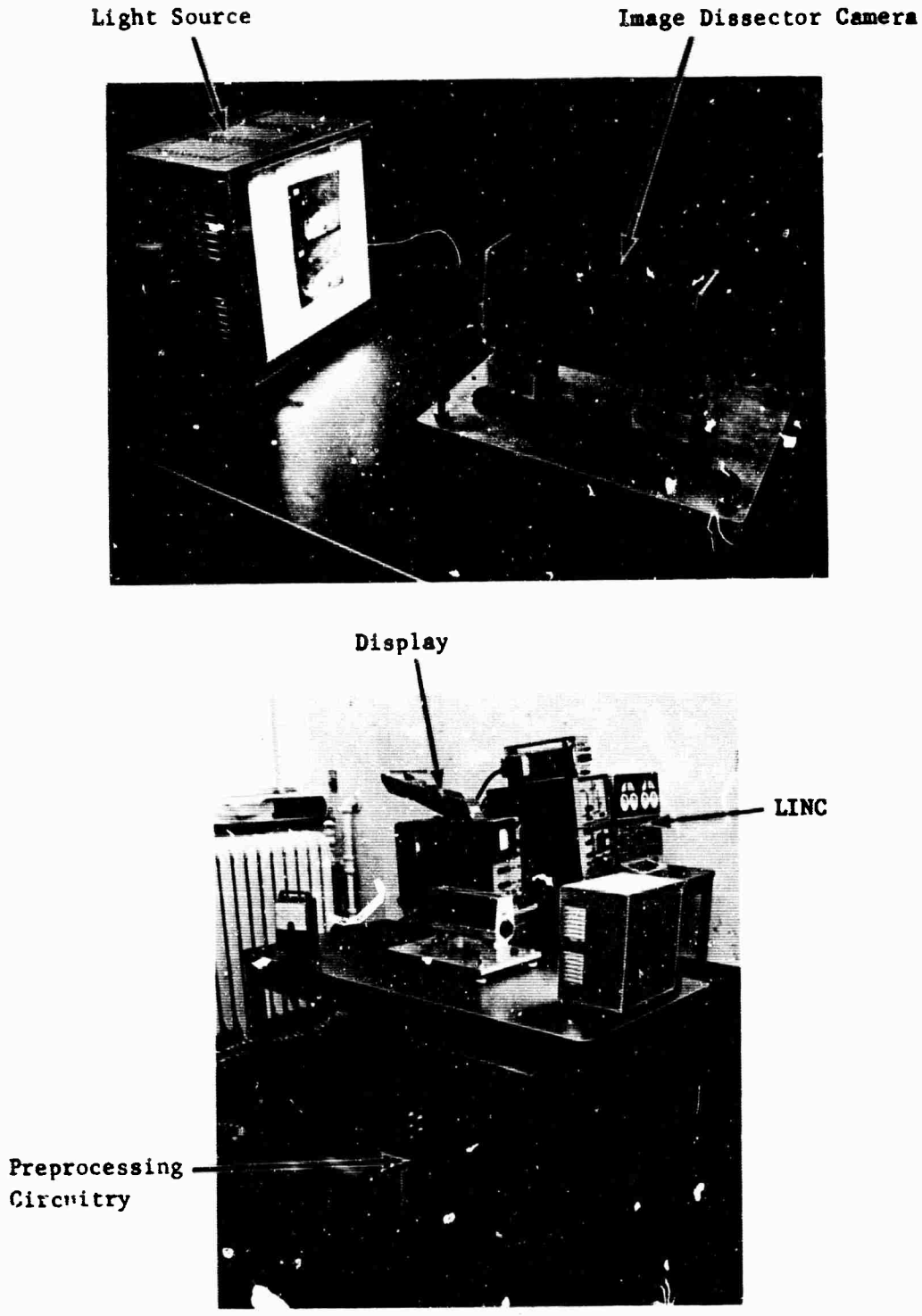

Figure 2. Photographs of the Apparatus

good reproducibility of the scanner, the input transparency functions as a read only memory. Thus, instead of digitally storing input densities for future reference, the scanner shifts to those points of interest and rereads them.

Some of the advantages of the LINC that tend to compensate for its slow running time and small storage capacity are the following: (1) accessibility, (2) availability, (3) simple programming format, (4) predesigned interfacing, and (5) output display. In the output display, a 561A Tektronix Oscilloscope is incorporated into the computer design whereby data can be displayed upon command.

The interfacing of the LINC to the other equipment of the system is accomplished with several analog to digital and digital to analog converters which are indicated in Figure 1. Both types of converters were constructed in conjunction with the LINC and operate by the execution of specific instructions in about sixteen microseconds.

Sixteen channels through which an analog signal may be digitized by the LINC are available. A sample instruction specifies which of these channels is to be examined and then linearly converts the line voltage to a digital number between $+177_8$ and -177_8. The voltage range for the analog to digital converters is plus and minus one volt, respectively, implying that for a least significant bit change in the digital number, a 0.008 volt change must be detected on the line. Eight lines of the sixteen analog to digital converters receive analog signals from within the LINC. Each is equipped with a potentiometer whose voltage may be altered by turning an external knob. With the internal lines numerous operations for the system may be performed, such as controlling the initial horizontal and vertical positions of the scanner.

One of the eight external channels samples the analog voltage signal representing the input image's density at a point. Therefore, a total of 256 input levels can be distinguished with the converter. This can be contrasted to the 64 gray levels often referred to in other similar systems.

The different digital to analog converters denoted in Figure 1 drive the scanner in the horizontal and vertical directions, modulate the intensity of the auxiliary oscilloscope and position a point for display on the scope. A d.c. output voltage from the converters is linearly proportional to a number in the accumulator when the proper instruction is executed. The voltage remains constant until the line is disturbed again with the instruction.

The scanning device is deflected by two eleven bit digital to analog converters with output voltages between zero and minus ten volts. For a least significant bit change of one, the voltage changes by 0.005 volts which does not restrict the resolution of the image dissector camera.

Two identical digital to analog converters are also employed for the auxiliary scope deflection. These are nine bit converters which means that approximately 250,000 individual display positions are possible on the oscilloscope's screen. The converter for modulating the scope's intensity has a zero to minus ten volt span operating from eight bits thus an output sensitivity of 0.04 volts per least significant bit change. The voltage from the converter is sometimes linearly attenuated or amplified to achieve the desired output density range. For more information concerning the LINC and its performance see References (20) and (21).

2.2 IMAGE DISSECTOR CAMERA

In the development of this image processing system, two crude scanning devices were investigated before the present scanner was finally incorporated into the system. With the earlier scanning devices other sections of the system were tested and improved so that not much modification was required when the more sophisticated scanning device was installed.

The temporary scanners were constructed first with a photodiode and later a bundle of noncoherent fiber optics both of which were mounted on the pen arm of an X - Y plotter which was driven by the LINC. A piece of clear plastic supported by the frame of the X - Y plotter supplied a foundation for positioning an input transparency for scanning. Either room light or a two bulb fluorescent desk lamp illuminated the transparency depending on the density.

These first scanning systems lacked resolution mainly because the apertures sensing the light were experimentally measured to be on the order of 50 mils in diameter. Besides the poor resolution, the X - Y plotter was rather awkward and slow because of the mechanical motion involved in scanning. But the limitations did not prevent the other sections of the image processing system from being checked, namely the computer programs, the analog processing and the output display.

The present image processing system functions with an image dissector camera, employing the F4011 Vidisector tube, and a d.c. panel fluorescent light source, both designed and constructed by International Telephone and Telegraph Corporation. The internal operations of this camera are shown in Figure 3 with a simplified diagram which will be explained.

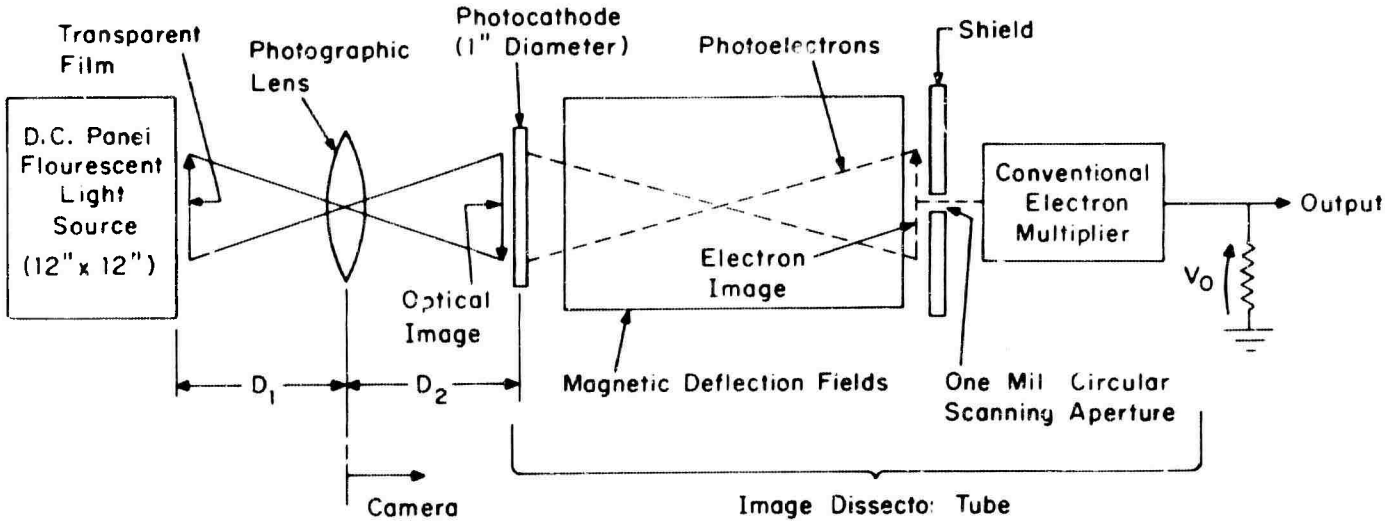

The electron image is focused on shield by means of a magnetic field.

Figure 3. Schematic of Internal Operations of Dissector Camera

The transparent film to be scanned is positioned on the surface of the panel fluorescent light source. The light is attenuated through the input film depending on the density and is viewed by the camera through a photographic f/2 lens with an adjustable aperture. The size of the input field is regulated by the distance, D_1, between the camera lens and the light source. For a smaller input field, the camera is moved closer to the light source; the reverse is true for a larger field. To focus the optical image on the cathode surface of the photo-tube, the distance, D_2, between the lens and the photocathode is varied.

The incident light projected on the photocathode causes a photo-emission of electrons to be released from the cathode which are then accelerated toward the shield by a potential difference between the cathode and the shield. The density of these emitted electrons in space is directly proportional to the light intensity of the optical image. Therefore, the optical image is transformed into an electron image which is projected and focused upon the shield by means of electrical fields.

The center of the shield in Figure 3 is shown with a circular aperture of one mil in diameter through which electrons from a specific point on the photocathode flow. The magnetic fields perpendicular to each other and to the electron image deflect the entire electron beam either vertically or horizontally. With the magnetic fields it is possible for the electron image to be scanned with the one mil aperture point by point, hence the name dissector tube. By displacing the entire electron image with respect to the aperture of the shield, mechanical motion is avoided. Therefore, good reproducibility of a scan is attainable.

Those electrons which pass through the aperture are amplified by a conventional electron multiplier. An electron current amplification of 5×10^4 is provided with this multiplier from which the electrons strike the anode inducing an instantaneous electrical current with a value corresponding to the aperture's electron density.

The magnetic deflection fields may be controlled by either an externally or internally applied d.c. or a.c. voltage. In either case, the voltages must be between zero and minus ten volts to operate the camera properly. Externally, the LINC supplies the necessary voltage through two identical digital to analog converters, one for the horizontal field and the other for the vertical field, to shift the electron image to a particular point. The output voltage from these digital to analog converters is linearly determined by an octal number between 0 and -3777_8 or 0.005 volts per least significant bit change. However, the resolution of the image dissector camera is theoretically 1000 points since the aperture is one mil in diameter and the diameter of the photocathode measures one inch. Therefore, neglecting any overlapping when scanning, a 0.01 volt change is required to shift the electron image from one point to an adjacent point. Any smaller voltage change would result in the "partial" scanning of the same point twice in one direction which in some cases may be an advantageous method of averaging.

To focus the dissector camera, the internal voltages are applied to the magnetic deflection fields; one is a sawtooth voltage with a variable frequency control and the other a constant voltage. The sawtooth voltage when applied to one of the magnetic fields continually sweeps the electron image across the scanning aperture in that direction,

while the constant voltage positions the sweep in the center of the other direction. If a transparent resolution chart is positioned in the field of view while the camera is internally sweeping and the camera's output voltage monitored on an oscilloscope, then the operator may focus the camera by adjusting D_1 and D_2 until the output waveforms appear sharp. With this method, any field size up to 12 inches square can be obtained.

An important feature of the image dissector camera is the nonstorage vidissector television camera tube, thereby allowing the scan pattern to be varied in any desired manner. While scanning an input image, the camera must be allotted approximately a delay of 100 microseconds to deflect the electron image from one side to the other in order that the output of the phototube may settle. However, this essential delay diminishes proportionately with the separation between scanned points until sampling adjacent points in which a delay of only one microsecond is required. These delays are not the limiting factors when speed is important since the average execution time for the LINC instruction is 16 microseconds and several instructions must be executed between scanned points. But with a much faster digital computer, these delays would have to be given consideration.

Besides the increase in scan speed and resolution over the earlier systems, the dissector tube's output is specified to be linear with input brightness. It is known that light intensity transmitted through a density is expressed by the relationship in Equation (1)

$$B = B_R 10^{-D} \qquad \text{Equation (1)}$$

where D represents the density and B_R is a constant representing the

light intensity for zero density over a short distance. If indeed the image dissector camera functions as a linear device with respect to intensity, then the output voltage from the camera should be directly proportional to light transmission.

To prove this, a calibrated Kodak Density Step Wedge with twenty-one steps was employed. After focusing the image dissector camera on one specific point in the field, the density wedge was manually shifted over the point one density step at a time. For each step the camera's output voltage, after linear amplification, was recorded and the data is plotted on semi-logarithmic graph paper shown in Figure 4. The straight line demonstrated that the camera's output voltage is indeed linearly proportional to the input intensity as stated.

To avert any light discrepancies the light uniformity of the fluorescent light source was measured with a computer program that scanned the light field, 12 inches square, with the dissector camera. The camera's voltage after analog processing was sampled at equal increments in the horizontal and vertical directions until the entire light field was traversed. Before scanning a reference point, a point in the center of the field, was sampled. After scanning, a matrix of octal numbers representing the scanned points and an octal difference between each of these numbers and the reference point was printed out. From the differences the most uniform region of the light source was ascertained to be a centered area of about six inches square with a maximum density variation of approximately plus or minus five percent. Therefore, when scanning an input transparency, as much of the uniform field as possible is exploited.

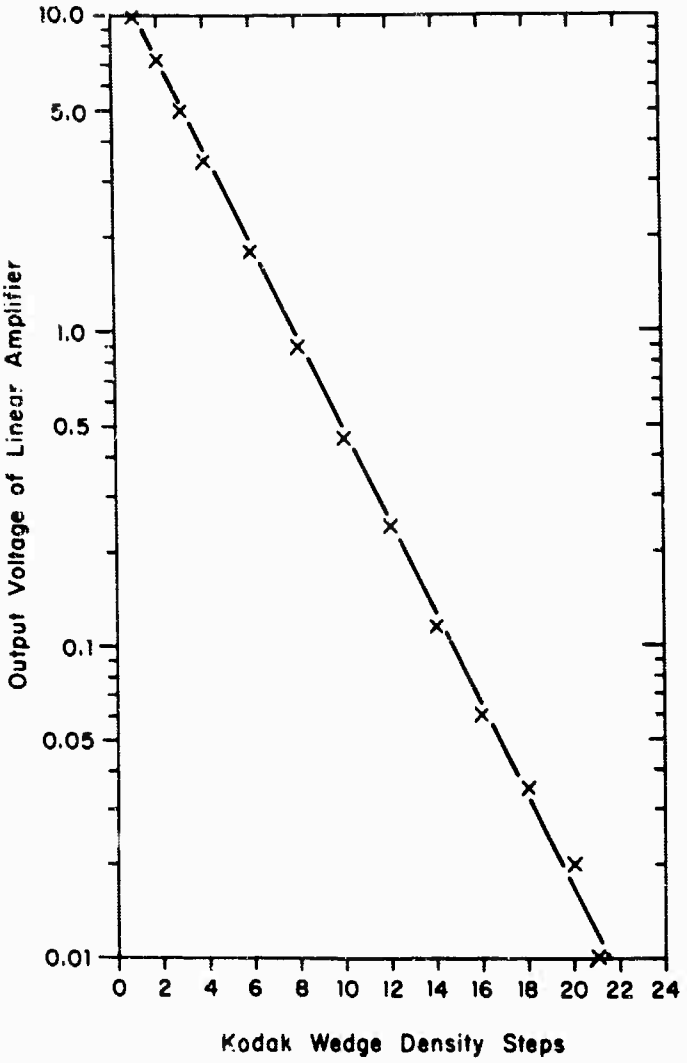

Figure 4. Linearity Test of the Dissector Camera-Preprocessing Circuit Combination

Table 1

Comparison of Present Scanning Devices

DEVICE	RELATIVE PERFORMANCE						
	SCAN SPEED	RESOLUTION	SIMPLICITY	LINEAR DYNAMIC DENSITY RANGE	PROGRAMMED SCAN?	SIGNAL TO NOISE	COST
IMAGE DISSECTOR CAMERA	MODERATE	MODERATE	EXCELLENT	EXCELLENT	YES	LOW	LOW
ELECTRONIC FLYING SPOT SCANNER	HIGH	HIGH	FAIR	EXCELLENT	YES	HIGH	HIGH
MICRODENSITO-METER	VERY SLOW	HIGH	FAIR TO GOOD	EXCELLENT	YES	HIGH	MODERATE
STORAGE TYPE TELEVISION TUBES	HIGH	LOW TO MODERATE	GOOD	FAIR TO GOOD	NO	MODERATE TO HIGH	LOW

Several other scanning devices are presently available and have been compared in Table 1. As the table indicates, increased quality involves a more intricate and more expensive device. The image dissector camera's characteristics are a good compromise between the microdensitometer and the electronic flying-spot scanner. However, the storage type television cameras, similar in many respects to the dissector camera, are extremely difficult to program scan because of their image retention property. Thus, the image dissector camera was preferred for this image processing system because its features best satisfied the requirements stated in the introduction.

2.3 ANALOG PREPROCESSING CIRCUITRY

In this image processing system some analog operations had to be performed on the image dissector camera's output voltage before being digitized by the LINC. Several different reasons for the additional circuitry included the following: (1) reduction of total scan time by replacing a digital process with an analog one; (2) amplification of the camera's signal; and (3) biasing of the input voltage to the analog to digital converter. The present system employs three basic optional analog processes, namely, low pass filtering, linear amplification and logarithmic amplification. The purpose and general operation of these analog processes are manifested in Figure 5 and will be explained.

In the original design of the image dissector camera, high and low pass filters, 50 KC and 5 KC bandwidths, were available for various statistical noise resulting from the camera's electron multiplier. However, these circuits were experimentally discovered to be rather noisy and unstable; therefore, a simple RC low pass filter was incorporated into the preprocessing circuitry. The low pass filter,

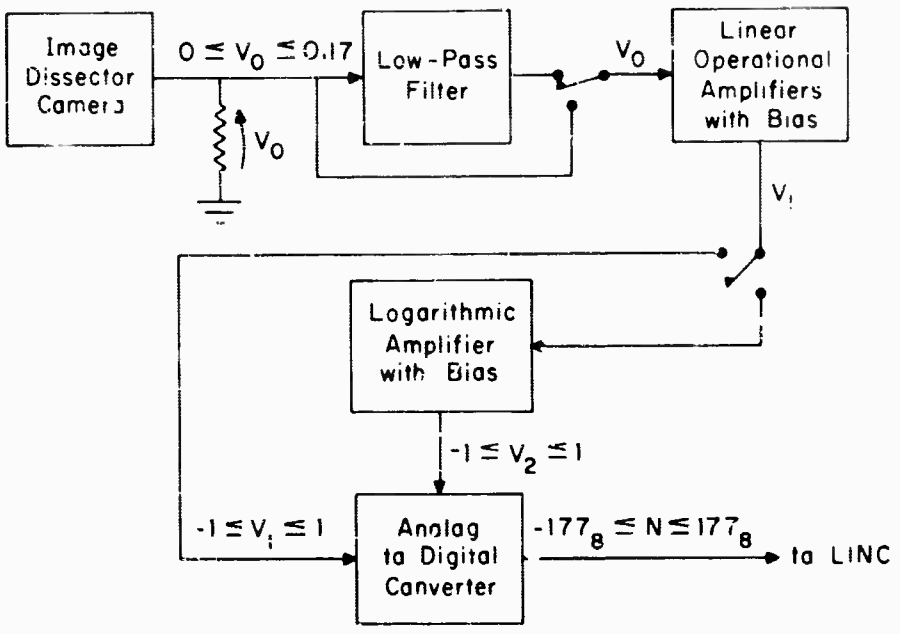

Figure 5. Block Diagram of Analog Preprocessing

which operated directly on the image dissector camera's voltage before any other analog processing, attenuated the signal at frequencies above the sample rate. If the sample rate was ever altered appreciably, a compensating modification would have to be made in the parameters of the filter or the filtering completely removed from the preprocessing circuitry.

The need for amplification arises from the fact that a maximum camera output voltage of 0.17 volts is observed when the camera is focused on the light source and the photographic lens is wide open. Closing the lens aperture reduces the input light intensity and consequently the output voltage, V_1. Furthermore, if the camera is shielded from all light, the voltage drops to zero volts. With these two boundary conditions and Equation (1), an expression closely representing the camera's response function with respect to input density, D_i, is resolved to be

$$V_1 = (0.17)10^{-D_i} \qquad \text{Equation (2)}$$

provided that for complete darkness D_i is large. With a 0.17 volt span, only ten percent of the analog to digital converter's two volt range would be utilized. The darker the input densities become, less variation in the camera's output voltage occurs as verified by Equation (2), thereby restricting the digital distinction in the darker densities.

To rectify this situation, two linear operational amplifiers with adjustable gain and a bias control were designed in cascade into the preprocessing circuitry as designated in Figure 5. The first of the amplifiers controls offset; the other, gain. With amplification

and offset, the entire sample span, plus one volt to minus one volt, of the analog to digital converter may be optimally exploited. The maximum output voltage for both amplifiers is plus or minus fifteen volts.

After adapting Equation (2) to include the amplifiers, the result is

$$V_A = G_1 10^{-D_i} + G_2 \qquad \text{Equation (3)}$$

where both G_1 and G_2 are constants. If the gain and bias settings are adjusted such that for zero input density the output equals two volts and zero volts for complete darkness, then Equation (3) becomes

$$V_A = 2\ 10^{-D_i} \qquad \text{Equation (4)}$$

neglecting G_2 because it is small. Some quantitative data verifying Equations (2) and (4) is plotted in Figure 5 on semi-logarithmic graph paper with the linear axis representing density increments of 0.15. Approximately fifteen density steps are detectable by the analog to digital converter when the camera's voltage is amplified. This is an improvement of about 1.5 over the unamplified camera signal which can be concluded from the curves in Figure 6.

With this preprocessing circuitry any two volt span, which describes the input densities about to be scanned, can be specified. If the input image's density spectrum is modified, then the gain and bias controls of the amplifiers can compensate so that the LINC is sampling from a voltage range representative of the input image. However, even with the linear amplification the darker densities are still compressed as illustrated in Figure 6, where density steps five to fifteen have voltages extending from 0.5 to 0.02 volts. Moreover, this voltage span

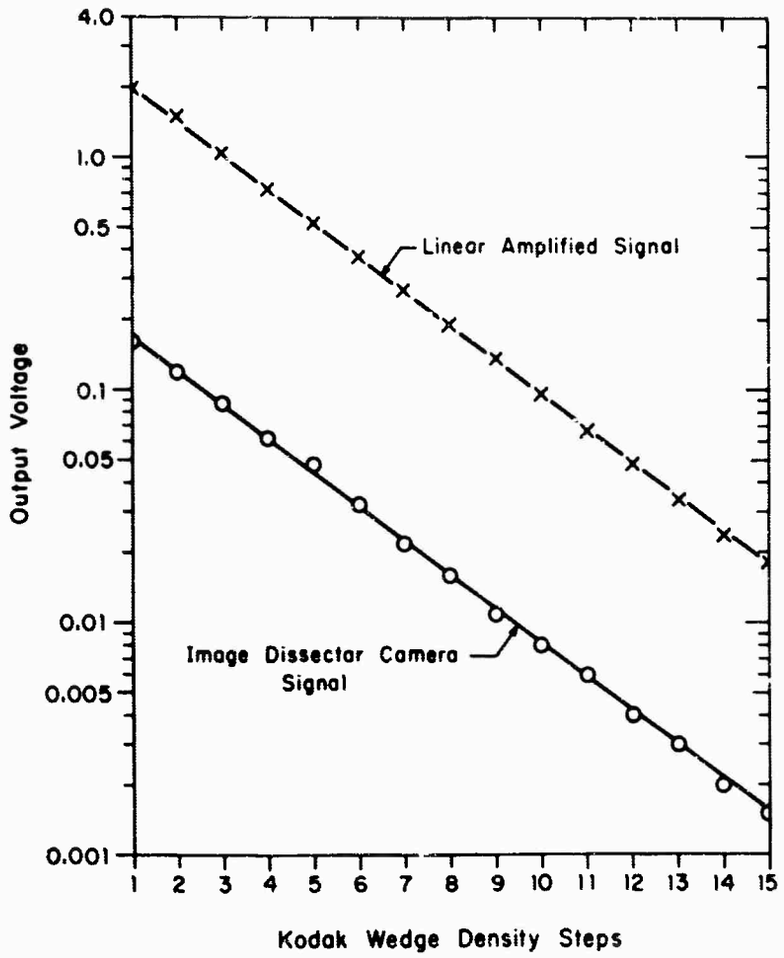

Figure 6. Experimental Comparison of Dissector Camera's Signal with and without Linear Amplification

condenses further when digitized. Augmenting the gain does not alleviate the problem if a wide input density range must be scanned. One solution is to implement a digital logarithmic function, but it would consume considerable running time. Besides, a quantization problem occurs at higher densities resulting from the analog to digital converter's sampling limitations For these reasons, an optional logarithmic amplifier was designed into the preprocessing circuitry as Figure 5 exhibits.

With the logarithmic amplifier operating on the output of the linear amplifiers, Equation (3) becomes

$$V_2 = \log V_A = K_3 D_i + K_4 \qquad \text{Equation (5)}$$

where K_3 and K_4 are constants. Both amplification and offset controls are available in order that any reasonable density range can be expanded over the required two volt range. The amplifier thereby supplies the analog to digital converter with a voltage that is directly proportional to the camera's input density.

The logarithmic amplifier's function was experimentally investigated with voltages simulating an exponential curve. To accomplish this, the image dissector camera's output for the Kodak Density Step Wedge was employed after linear amplification. For each input voltage to the logarithmic amplifier the corresponding output voltage was recorded and later plotted in Figure 7, along with the input curve. The stability of the logarithmic amplifier becomes critical as the input voltage approaches zero volts, or in other words as the input density increases. But, this happens for those densities above 2.7 and hence does not affect most optical images. If the same procedure is employed several

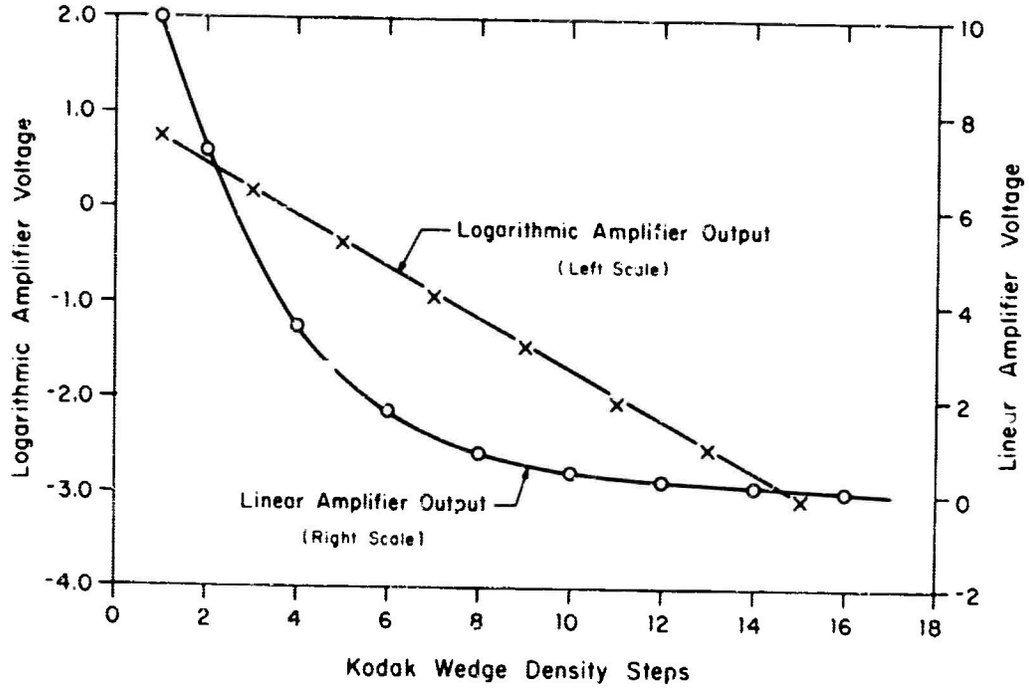

Figure 7. Comparison of Logarithmic and Linear Amplifiers' Density Response

times for the same input curve but with various gain and bias settings on the logarithmic amplifier, then the resulting curves are those illustrated in Figure 8. The curves depict the fact that varying the gain and bias settings regulates the input voltage range to the LINC and consequently, the density spectrum for sampling.

The circuit diagram of the preprocessing circuitry is presented in Figure 9 where the filtering, biasing, linear and logarithmic constituents are designated by dotted lines.

2.4 DISPLAY EQUIPMENT

The display of the image processing system is extremely critical because the output picture provides the best means by which the whole system's operations can be evaluated. From the final product the human operator can conclude what parameters should be adjusted in either the digital or the analog portions of the system to optimize the output picture. Therefore, the characteristics of the display apparatus had to be carefully examined in order that a satisfactory multilevel density display might be developed. Figure 1 denotes the display part of the system consisting of an auxiliary [illegible]ope, a camera, film and in some cases analog post processing circuitry. The procedures and results involved in researching the equipment will be presented in the remainder of the section.

The 561A Tektronix Oscilloscope servicing the LINC as display could not easily be adapted for the system's output display device. The main reason was that the tube has a long persistent phospher for continually displaying large amounts of visual information without too much flicker. Therefore, another 561A Tektronix Oscilloscope coupled to the LINC's scope functions as the system's display. A P31 standard

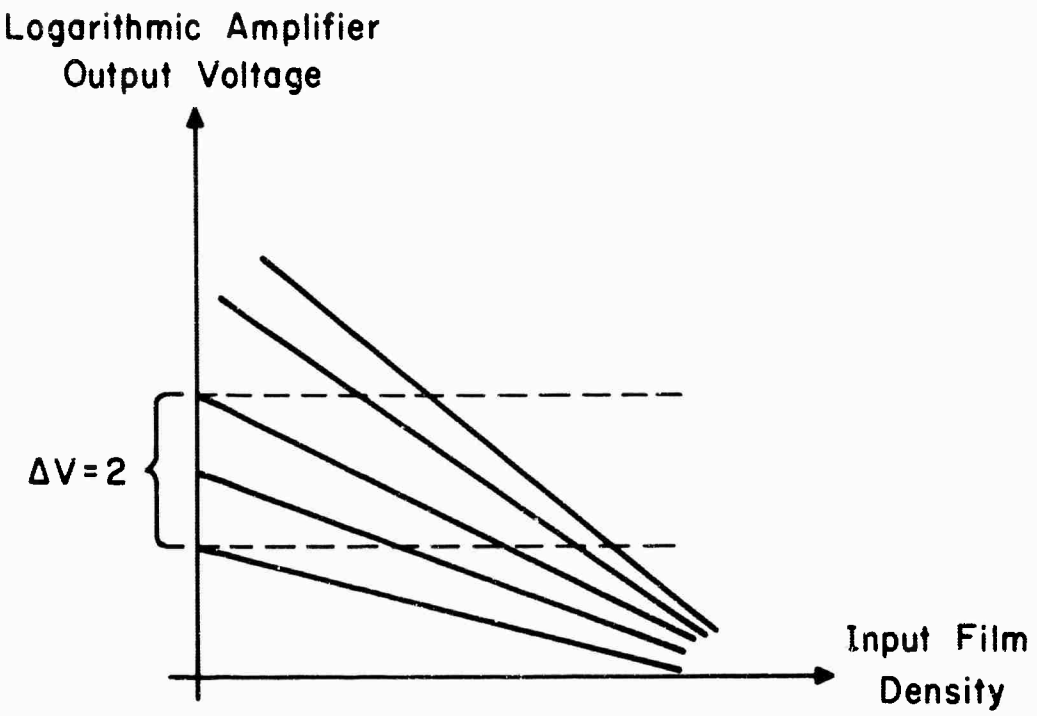

Figure 8. Logarithmic Amplifier Response for Various Gains

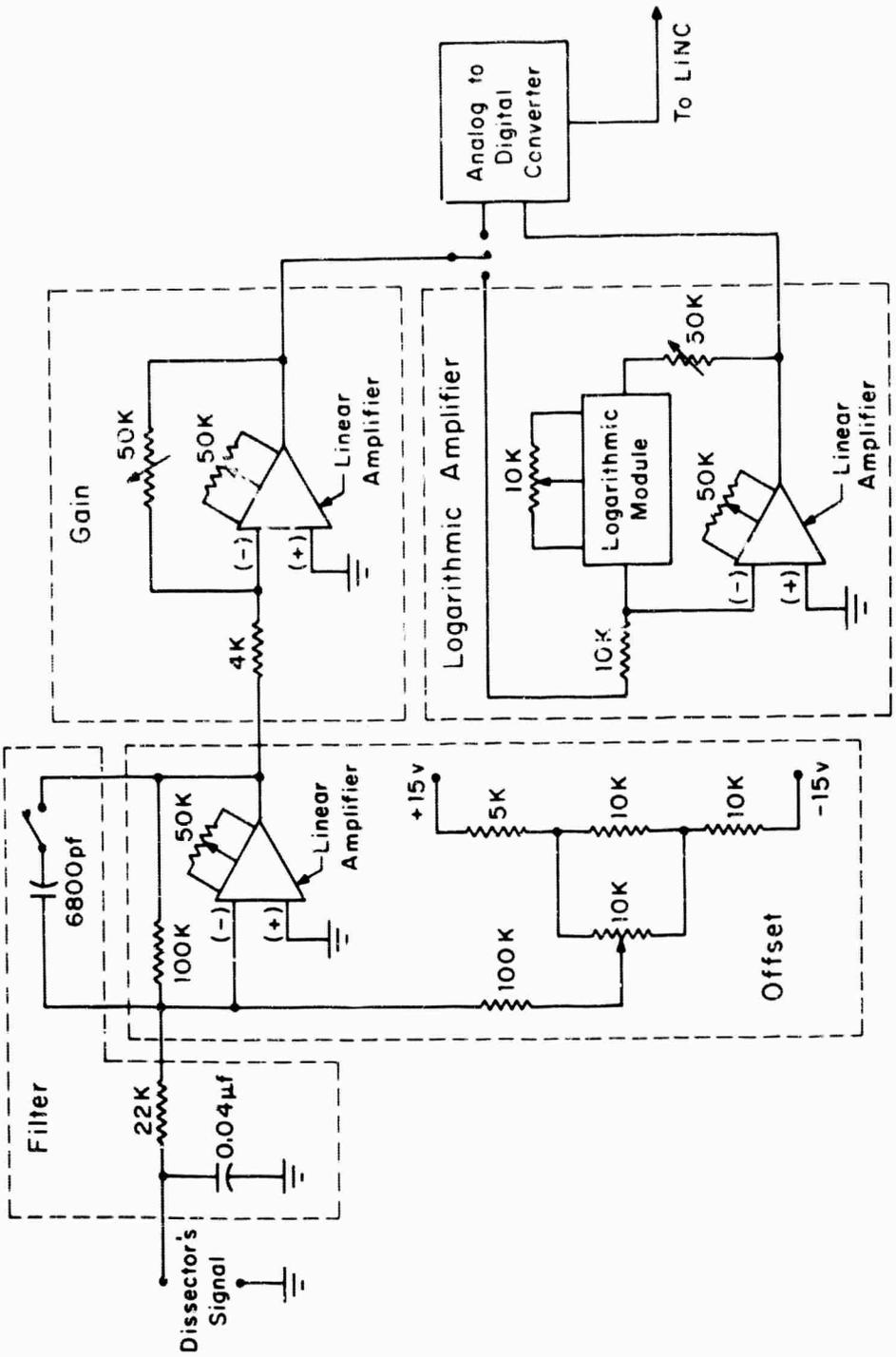

Figure 9. Analog Preprocessing Circuit

phospher tube which has a relatively short persistency and a spot size of approximately ten mils in diameter was installed in the auxiliary oscilloscope.

Being slaved to the LINC's scope, the auxiliary oscilloscope receives the same horizontal and vertical deflection signals. To intensify a point on the supplemental oscilloscope, the display instruction for the LINC's scope must be executed. Thus, whatever appears on the LINC's oscilloscope will identically appear on the auxiliary scope, the only difference being the degree of intensity.

Intensity modulation or z-axis modulation is accomplished by applying a negative voltage pulse to the tube's cathode. The cathode can sustain any voltage change between zero and -30 volts; however, the logarithm of the scope intensity is not a linear function of the voltage as is desired. The method for ascertaining the display function and the results will be outlined a little later in this section.

The voltage to modulate the intensity is supplied from the LINC through a digital to analog converter described earlier. The display procedure follows the sequence for applying a z-axis voltage, displaying the point and resetting the z-axis voltage to zero, thereby pulsing the cathode of the oscilloscope. The series entails six LINC instructions with a total execution time of 9b microseconds as compared to two LINC instructions with a total execution time of 48 microseconds for a two level output display.

A Polaroid camera with a f/2 lens is mounted on the auxiliary oscilloscope for photographing the output image. Two kinds of Polaroid film have afforded satisfactory results, namely Polaroid Land Film Pack (Type 107) with 3000 speed and Polaroid Land Projection Film (Type 46-L)

with 800 speed. The former film is a black and white positive, ten second development, with a density extending from 0.02 to 1.6; the latter is a positive transparency, two minute development, with a density ranging from 0.05 to 2.4. If possible, the output film's density range should be at least equal to if not greater than the input film's density spectrum to avoid compressing a wide input density range into a narrow one. One reason for selecting the fast development films was simply to obtain the output picture quickly and thereby retain as much on-line capability as possible.

Both films have a nonlinear characteristic of output density versus input brightness of film (22). A somewhat linear region exists over the middle half of the quoted density spectrum, but it is quite impractical to restrict the display to this narrow portion. Thus, in endeavoring to devise a linear display, the nonlinear film characteristic was included.

Besides the film's nonlinearity, several other parameters of the films were considered. The transparent and print films have a resolution of 22-28 and 32-35 lines per millimeter respectively, which is not a limiting factor of the system. Film graininess and uneven development are two other disadvantages of the transparent film that have to be realized when analyzing results. However, none appear to be too objectionable at the present and are about the best that can be employed without going to a longer development time.

Before proceeding to resolve the display function, the uniformity of the display had to be investigated. This was done with a computer program that displays forty rectangles of equal dimensions over the entire screen and all at the same intensity. Each rectangle was

exposed on transparent film and later a voltage proportional to the density of each rectangle was measured with the image dissector camera in a similar method used for measuring the densities of the Kodak Density Step Wedge. The voltages were then compared for discrepancies, and tolerances using the center rectangle as the normal were determined. Several such tests covering a wide range of the scope's intensity were performed, and it was concluded from the results that an approximate three by four inch area centered on the screen offers the most uniform display region, where the error is limited to a maximum of plus or minus ten percent. The exact reasons for the nonuniformity are not presently known, but it probably can be attributed in part to both the nonuniformity of the film and scope's intensity.

To discover the output display's characteristic, a simple computer program using the display sequence was implemented to generate a density step wedge on the auxiliary oscilloscope's most uniform region. The voltage pulsing the z-axis was equally incremented for each step that appeared on this output wedge. The computer generated wedge was exposed on the transparent Polaroid film from which density measurements could be attained. Several wedges were displayed with different exposures and initial intensity settings until most of the film's density spectrum was explcited.

The procedure for measuring the densities with the image dissector camera was identical to the one described earlier in this chapter. The image dissector camera's output signal was processed with the logarithmic amplifier so that a plot of the results could be made on linear graph paper. The logarithmic amplifier was adjusted using the Kodak Density Step Wedge to comprise the densities between 0.05 to 2.40

or steps one to sixteen. However, achieving this density range on the oscilloscope was rather difficult. A plot of the logarithmic amplifier's output voltage versus input density steps is presented in Figure 10.

With preprocessing circuitry initialized, the computer steps were measured and recorded. A representative curve for a typical set of data is shown in Figure 11. The computer steps have been plotted in equal increments because the LINC numbers supplying the voltage to the oscilloscope were equally augmented between steps. By comparing this curve with the Kodak Density Step Wedge, it can be determined whether or not the film's density range is being efficiently exploited. For example, step five of the computer wedge corresponds to a logarithmic voltage of approximately -0.64 volts. Referring to the same voltage on the Kodak Wedge curve, density step 6.6 is discovered; therefore, step five represents a density of 0.99. The entire density span of the computer wedge is similarly ascertained to be 0.58 to 1.92.

To compensate for the breaks in the output density curve, a break amplifier was constructed with an operational amplifier and a diode. However, to produce a satisfactory linear output density curve with this amplifier required considerable experimentation with circuit parameters each time the apparatus was set up. It was later decided that if a linear output density curve was to be realizable, most of the breaks occurring in the original curve would have to be corrected. But with analog circuits the procedure would entail adjusting more parameters and hence, more time experimenting until the desired output curve is finally attained. Therefore, it seemed reasonable to consider a digital procedure in which any number of the breaks in the original curve

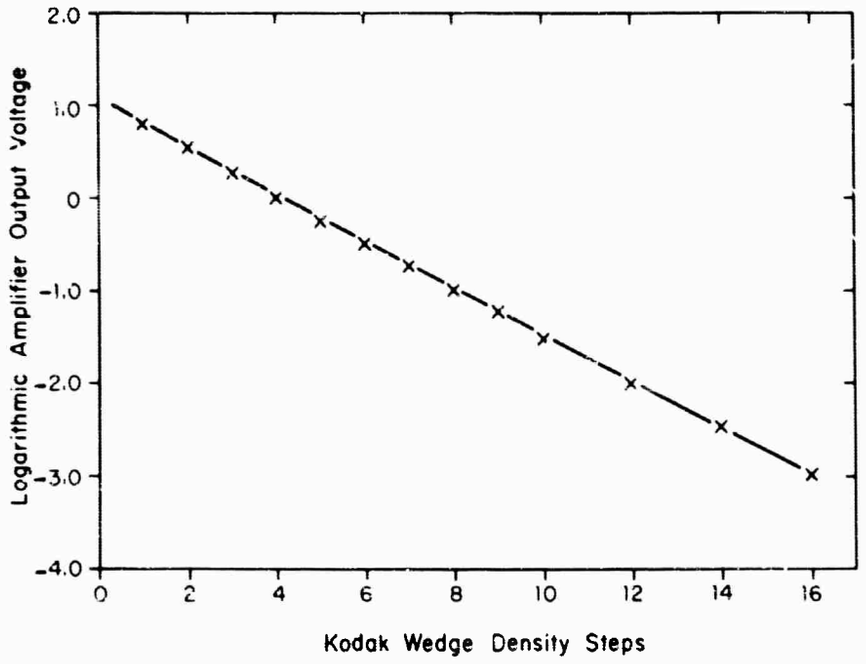

Figure 10. Dissector Camera's Density Response After Logarithmic Processing

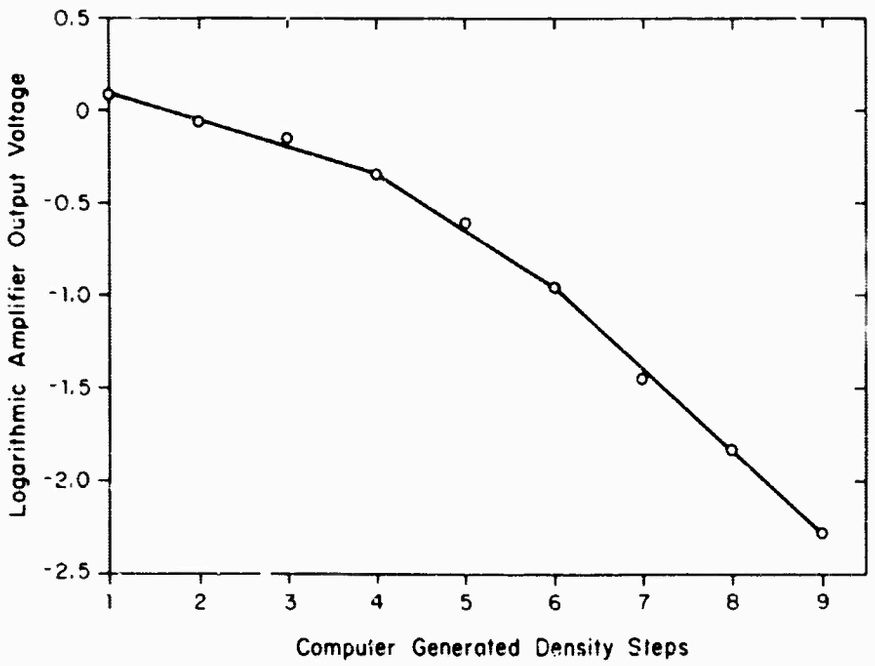

Figure 11. Uncorrected Computer Generated Step Wedge

could be compensated. Because this method constitutes a basic computer program, its discussion will be postponed until such programs are presented.

Sometimes a simplified two level display adequately services the image processing system. In such cases, a 564 Tektronix Storage Scope operating in the storage mode enables the operator to view the output image as displayed. Another advantage with the storage scope is that pictures do not have to be photographed with every scan as in the z-axis modulation procedure thereby saving exposing time as well as film. However, one disadvantage is that the scope tends to smear thus degrading the quality and resolution of the overall output picture. Ideally, a multilevel storage oscilloscope without smearing would best serve this image processing system. Such oscilloscopes are presently available, however, at a very high cost and with a significantly smaller gray scale range.

3. COORDINATING PROGRAMS

Several different LINC programs have been designed to coordinate the operations of the image processing system. The programs determine the procedures for scanning the input image, processing it and displaying the output picture. Each method has been programmed into separate subroutines and respectively referred to as the Scan, Digital Processing and Display routines. Also two additional subroutines, Histogram and Computer Wedge, are available to assist the operator in checking the performance of the system during a scan. The flow chart in Figure 12 indicates the general format of a coordinating program and the order in which the different subroutines would normally be executed. The Scan routine controls the systematic manner in which the input image is viewed by the dissector camera and then each input point is digitally processed according to some predetermined procedure. If operating, the Histogram subroutine offers a means of inspecting the performance of the preprocessing circuitry and digital processing. Next, a point is displayed on the supplemental oscilloscope at a specified intensity. The program continually cycles through these subroutines until the scan is terminated after which a computer generated step wedge is displayed on the output picture to test the display. This chapter will focus primarily on the basic subroutines, Scan and Display, with a brief explanation of the system's analyzing routines, since these subprograms vary only slightly between two coordinating programs.

3.1 SCAN PROGRAM

The scan subroutine, which is outlined in a flow chart in Figure 13, linearly moves the scanner through the input field sampling the

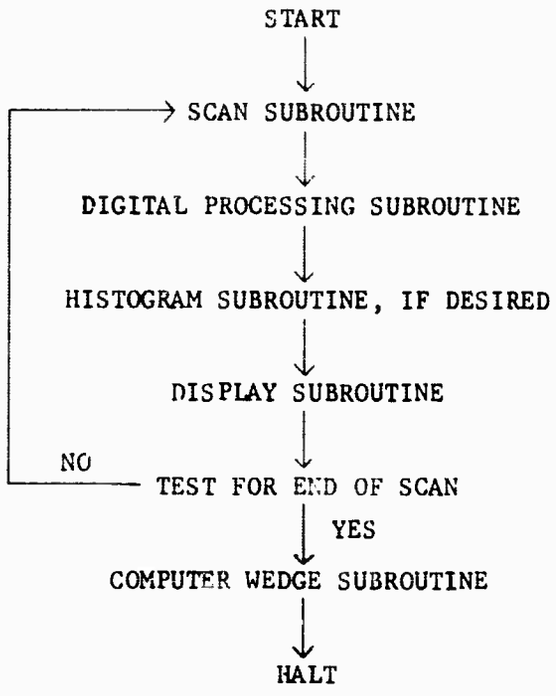

Figure 12. Fundamental Flow Chart of a Coordinating Program

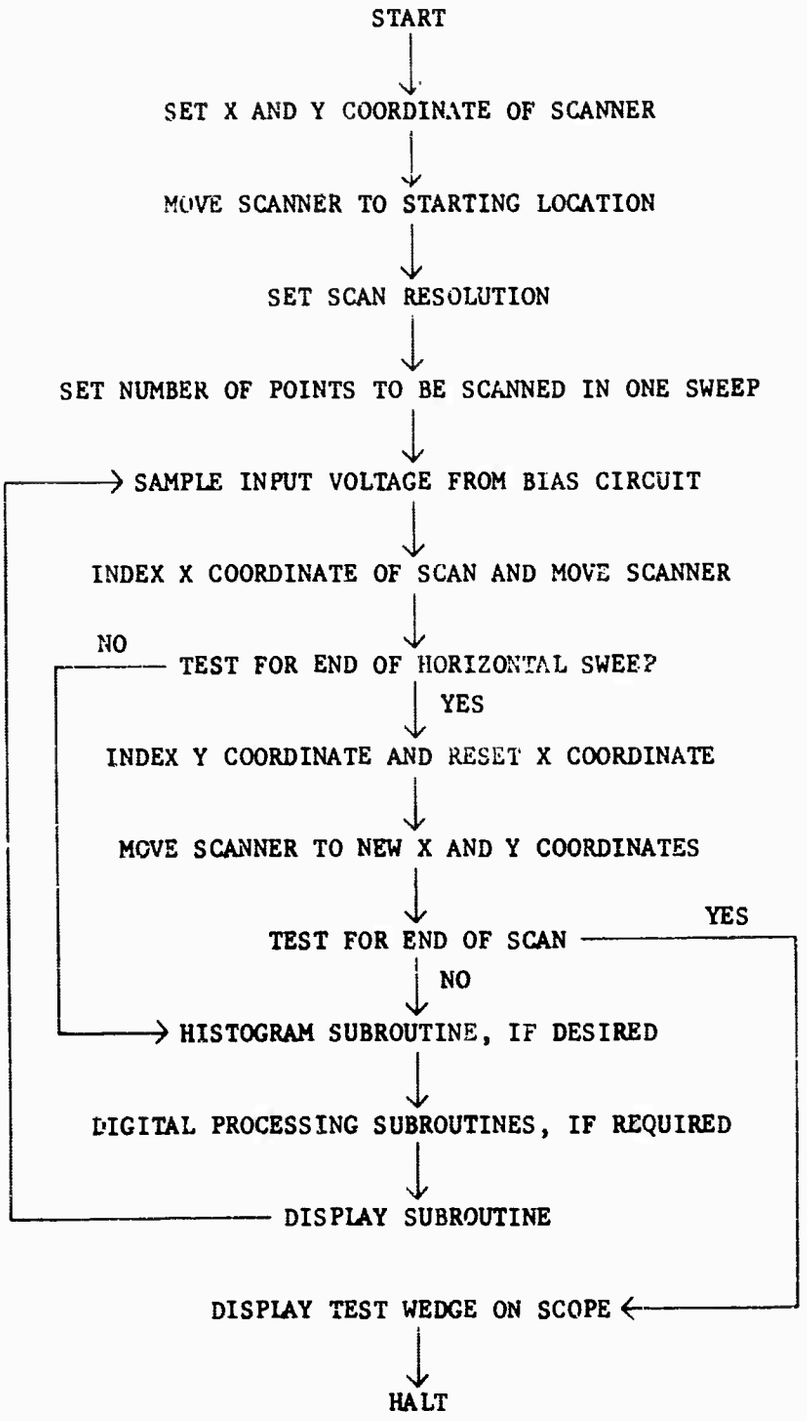

Figure 13. Flow Chart of Linear Scan Subroutine

input density at destinated increments. But before the scan commences, an initial location in the image dissector camera's field is selected through the digital to analog converters. Also, the number of points to be scanned in the horizontal sweep and the scan resolution must be set into the LINC. Scan resolution is defined as the voltage increment that must be applied to the scanner to yield a particular distance separation between adjacent scanned points. After these initializations are completed and assuming that the remainder of the system is properly set up, the scan operation commences on a signal from the operator.

Upon sensing the operator's command, an input voltage, corresponding to the input density at the scanner's present location, is sampled through the analog to digital converters whereby the signal is digitized and stored in the computer for digital processing. The scanner is then shifted to the horizontally adjacent point according to the present scan resolution. Next, a test is performed to see if the horizontal sweep is completed. If not, the Digital Processing and Histogram routines are executed as shown in the flow chart of Figure 13. However, if the sweep is completed, the scanner is indexed to the next adjacent line and relocated to its original horizontal location. Because of the limited display field a test is executed to decide if the field has been exhausted; and if not, the subroutine proceeds through the Digital Processing and Histogram subprograms until the Display is encountered. Otherwise, a Computer Wedge is displayed and the program terminated. After executing the Display subroutine, the sequence of operations is repeated until either the display field is exploited or the operator commands a halt.

In the selection of the above linear raster scanning procedure, simple programming and scan speed were the principal considerations.

If a complex programmed scan is designed, a slower scan speed results. Moreover, the programming involved for such a scan is compounded because the Scan and Display subroutines are very similar. Hence, with a linear scan more running time can be allotted for digital processing rather than scanning and displaying.

A vertical sweep, similar to the horizontal, could easily have been programmed but the results should be of the same quality independent of the sweep direction. One reason such a scan is not employed is that the LINC's indexing operation requires a few additional instructions to index the Y coordinate of the display. An example of an output from a horizontal raster scan is exhibited in Figure 14. The scan resolution was set such that most of the dissector camera's field of view was scanned. The print of Figure 15 was then obtained by altering the scan resolution and not the camera's field, thereby demonstrating that various degrees of resolution are possible without having to adjust the focus of the camera.

Other scans have been specially devised for more intricate digital processing in which neighboring information on the input image is utilized. The scans usually entail scanning the same point several times or storing immense quantities of data in memory. The extra time expended in rescanning or storing data make these types of digital processing much longer in scan time.

The Histogram subroutine is shown in the flow charts of Figures 12 and 13 to be optional depending on the operator. Its general purpose is to furnish information on the input and output densities of the scan from which the parameters of the preprocessing circuitry and Digital Processing subroutines can be optimally adjusted. Two types of histograms,

Figure 14. Example of Processed Image Produced by Horizontal Raster Scan

Figure 15. Improved Resolution by Digital Means

input and output, are available for examination and are graphically displayed upon command. The data for the histogram is accumulated during a scan thereby measuring the dynamic operations of the scanner and the preprocessing circuitry. Essentially, the subroutine computes the number of times each possible digital input and output density occurs in the entire scan.

When the input histogram is displayed, the vertical axis represents the count of each density; and the horizontal axis, the densities. The maximum number of points that may appear is 256 which is the capability of the analog to digital converter. From the histogram display it is easily determined what adjustments in the preprocessing circuits must be made to efficiently utilize the two volt span of the converter. The output histogram is similarly analyzed except the digital processing parameters are corrected. Furthermore, either one or both of the two histograms can be permanently recorded on the output picture for future reference.

A good example of an input histogram is presented in the print of Figure 16. The picture was obtained by scanning a Kodak Density Step Wedge with analog preprocessing (logarithmic) but no digital processing except the display correction. As the picture illustrates, one of the density steps was masked from the scanner. In order to read the histogram the entire picture should be rotated 90 degrees clockwise. The highest densities are manifested on the histogram to the left and the lower densities to the right. The heights of the peaks are proportion to the number of occurrences for the various input densities. Each peak corresponds to a density step on the wedge; however, a gap exists where the masked density would have occurred had it been visible to

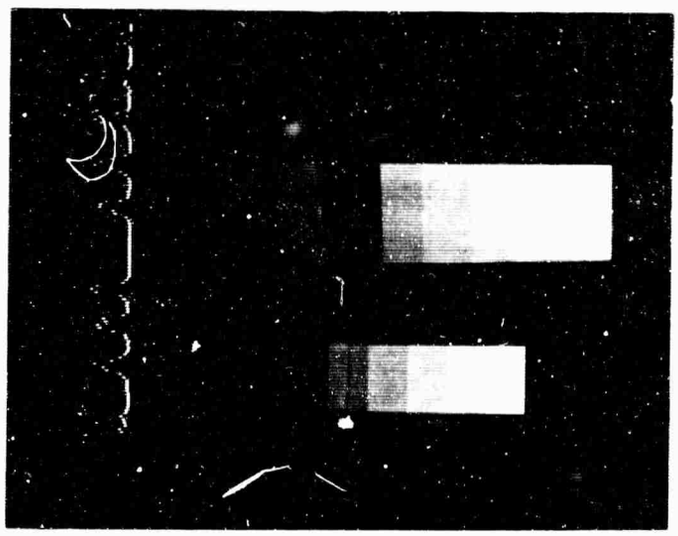

Figure 16. Experimental Data Representing the Histogram Subroutine's Function

the scanner. Whenever the logarithmic amplifier is employed the voltage to the LINC is directly proportional to the input density as was previously proven. Since the density increments of the wedge are equal, the distances between two peaks are equal. Also the height of each histogram peak is approximately the same indicating that each step was equally scanned in area.

3.2 DISPLAY METHODS

Several techniques were considered in attempting to attain a satisfactory multilevel display. Two significantly different methods, Dot Matrix and Intensity Modulation, fulfilled the basic requirement of providing discernible levels of gray and therefore were incorporated into separate computer subroutines. As previously mentioned, the display subroutines are entered with a predetermined digital output density value which has been digitally computed by a particular process. From the value the display routine must transform it into a corresponding density on the output image. The Dot Matrix accomplished this by displaying various dot patterns while the Intensity Modulation employs voltage modulation at the z-axis to control the oscilloscope's intensity. In the following two sections the subject matter will comprise a description and analysis of these two display subroutines.

3.2.1 Dot Matrix Technique

The Dot Matrix subroutine involves an n by n matrix display for each of the scanned input points that are to be presented. A multilevel density display could then be achieved by varying the number and arrangement (point code) of points displayed in the matrix. In designing the program, the grid size and point codes that best exhibit distinguishable levels of gray had to be specified.

When deciding on the size of the matrix, two opposing factors must be investigated. Logically, a larger matrix is capable of producing more discriminate densities than a smaller one since more possible point codes exist. But the LINC is presently restricted to a 500 by 500 point display field. For a n by n matrix, n^2 points of the display are used for each output element; consequently, the available field diminishes proportionately as the matrix dimension increases; therefore, a compromise must be reached between the number of different levels of gray and the matrix size. Also, only a square, n by n, matrix could be employed, otherwise a distorted output picture would result.

After establishing a grid size, various point codes are considered in order to discover as many distinct levels of gray as possible. Usually this entails an exhaustive search whereby different point patterns are displayed and then compared. First, several point codes are displayed in which only the pattern is varied while the number of points remained constant. Some of the possible codes are selected for future consideration and then the point count increased by one and the method executed again until the matrix field is exhausted. Next, the potential density codes are compared; however, an objective comparison strictly on a density basis is not always possible because the differences are sometimes a result of the pattern appearance and not the density. Finally, the best point codes are programmed into the display subroutine.

The fundamental operations of the Dot Matrix subroutine are presented in the flow chart of Figure 17. The subroutine is entered with the desired digital output density value which is a number between zero and 377_8. Initially, the operator divides this range into discrete output levels of gray where each level is represented by a particular code. The

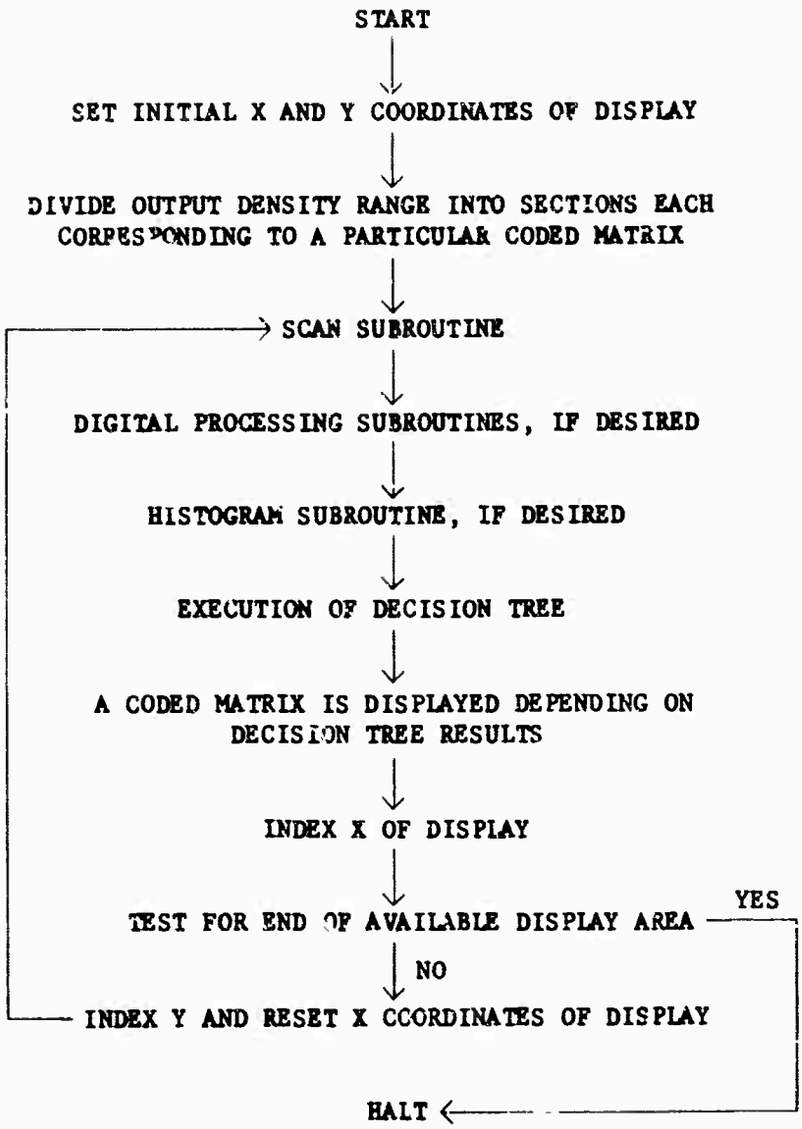

Figure 17. Flow Chart for Dot Matrix Display

operation is facilitated by the output histogram from which reasonable intervals can be determined. A decision tree is programmed from the division settings whereby the proper point code is computed and displayed before proceeding to scan the next input point.

To procure a better understanding of the Dot Matrix subroutine an example will be presented. The matrix dimension and point codes will assume to be such that only six discernible output densities are available. This means that the calculated output density range (0 to 377_8) can be separated into six intervals (T1, T2, ...T6) as is demonstrated in Figure 18. Any digitally processed output density must occur within one of these divisions and therefore displayed by the corresponding coded matrix (L1, L2, ...L6) assigned to the range by the operator. For each calculated output density (T) the decision tree, also shown in Figure 18, is executed with the result that one of the point patterns is displayed.

A picture of George Washington produced with the Dot Matrix is presented in Figure 19. As the prints illustrate, the difference in point patterns appears to differentiate two regions rather than the densities themselves. Also an overall roughness exists in the picture because the matrix is too large by comparison with the size of the field displayed. This may be improved with a larger digital analog converter and newer model scope. The International Telephone and Telegraph Corporation has developed a multilevel storage scope but it is rather expensive. Although the picture of George Washington is not of high quality, it may be useful when it is necessary to view the picture as it is scanned.

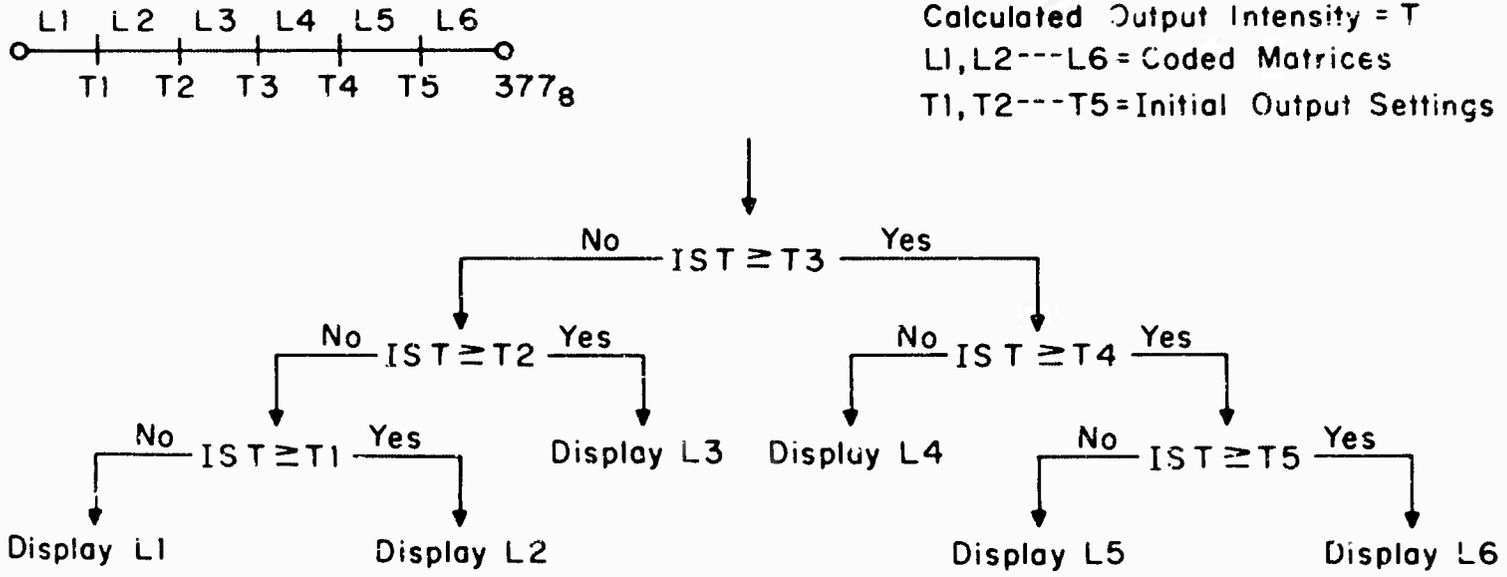

Figure 18. Decision Tree Manifesting the Procedure for Determining the Matrix to be Displayed

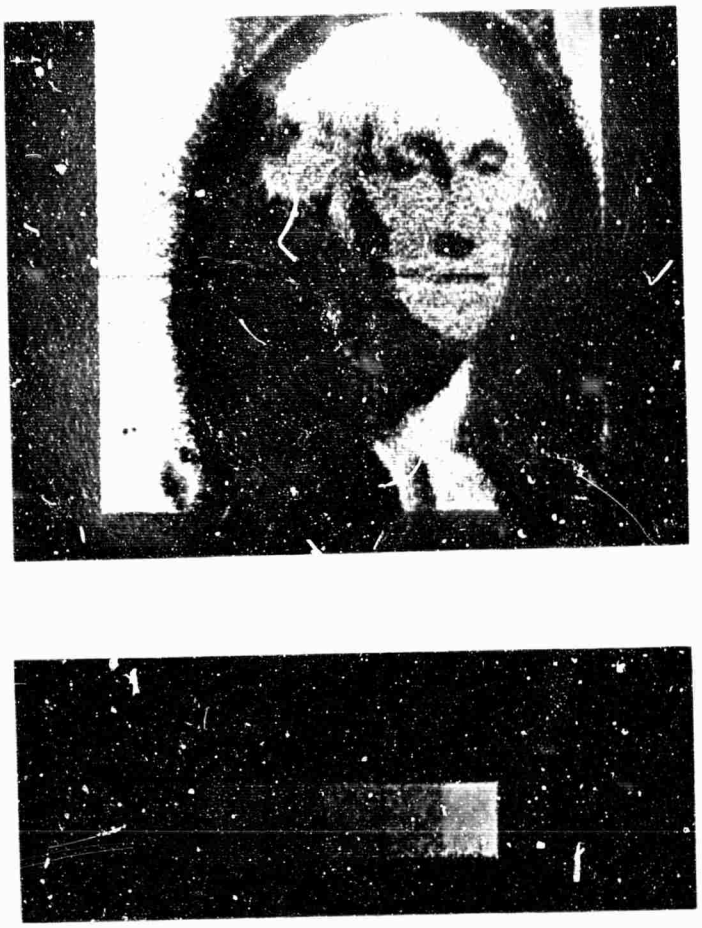

Figure 19. Example of the Dot Matrix Display Capabilities

3.2.2 Intensity Modulation Procedure

An alternative to the dot matrix display is to modulate the intensity of the auxillary oscilloscope by applying digitally generated voltage pulses to the cathode. In the design of such a method, the output density spectrum and a linear relationship between the density and the s-axis voltage were the primary considerations. A computer generated density wedge with the intensity modulation technique was developed to experimentally examine these two characteristics and at the same time provide a means of calibrating the display apparatus. This section will discuss the subroutines for displaying a computer wedge, for correcting the display's nonlinearity characteristic and for displaying an output picture.

In the programming of the computer generated density wedge, provisions were implemented for externally controlling the positioning of the wedge on the oscilloscope's screen, the dimensions of the steps, the number and the digital value corresponding to the s-axis voltage. The flow chart representing the initialization of these conditions and operations of the program is shown in Figure 20. To vary the scope's intensity the cathode is pulsed with a negative voltage as outlined in Section 2.4. An example of a digital wedge with nine levels of gray is presented in Figure 21 where each step is generated by equally incrementing the voltage applied to the cathode. For testing purposes the computer wedge is displayed on the most uniform area of the screen, which was specified in an earlier section.

A wedge similar to the one in Figure 21 was exposed on the transparent Polaroid film and the density of each step was measured.

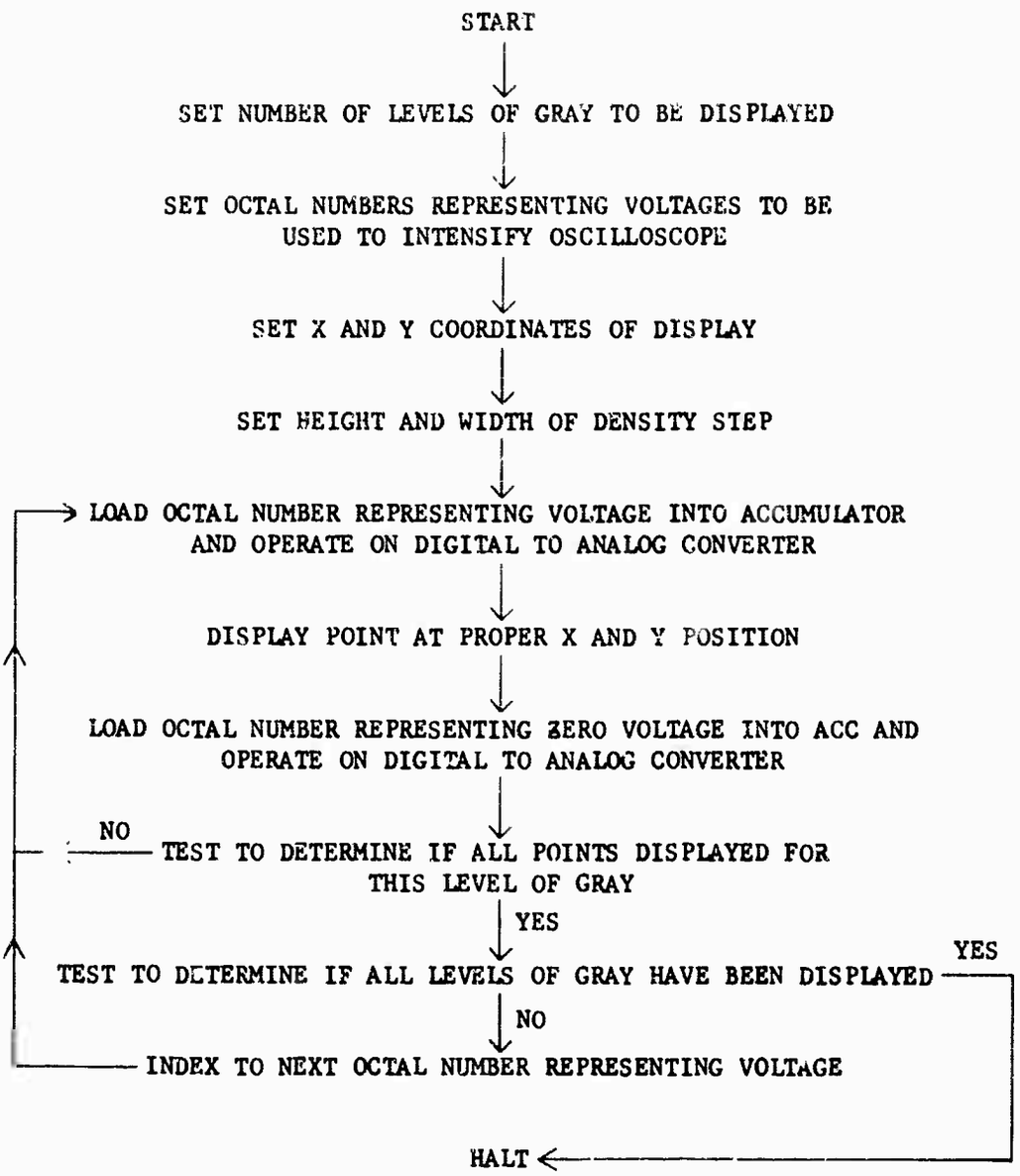

Figure 20. Flow Chart for Density Wedge Display

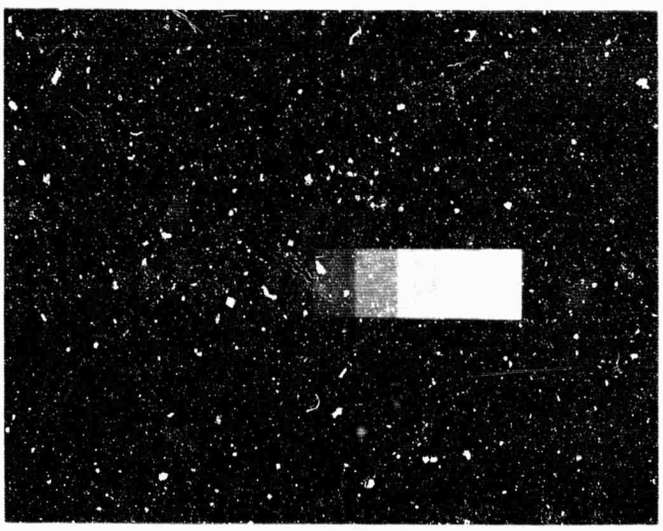

Figure 21. Typical Computer Generated Wedge Produced by Modulating the Intensity

The procedure and results of such a measurement were previously described in Section 2.4 and as the graphical representation of the data in Figure 11 indicates, several discontinuities were observed. The first attempt to correct the break points engaged an analog process, a break amplifier, which did succeed in biasing the breaks such that a linear relationship was obtained. However, each time the system was set up, the parameters of the break amplifier would have to be recalibrated; therefore, a digital method was devised which would in effect perform the identical correction but require less adjusting.

A facsimile of an output curve for the computer wedge is shown in Figure 22. The LINC numbers have been offset by -200_8 and complemented to avert the complication of negative numbers in computations and programming. As a result, the minimum input and output densities correspond to 377_8 and the maximum to zero; henceforth this terminology will apply to digital densities unless otherwise specified. Each of the discontinuities on the curve have been labelled with the actual (A) digital values. Using the experimental curve as a reference, a desired output density curve, a straight line, can be fitted. This line must originate at the same coordinates as the reference for programming purposes; however, no single theoretical curve appears to be optimum although the density spectrum should be similar to the reference. One of the many possible lines has been drawn in Figure 22 from which the desired (D) digital values are specified by the density break points of the experimental curve. Now for a particular actual output value the ideal output value can be determined from two curves.

To more fully understand how this is accomplished a curve shown in Figure 23 better manifests the relationships between the two curves

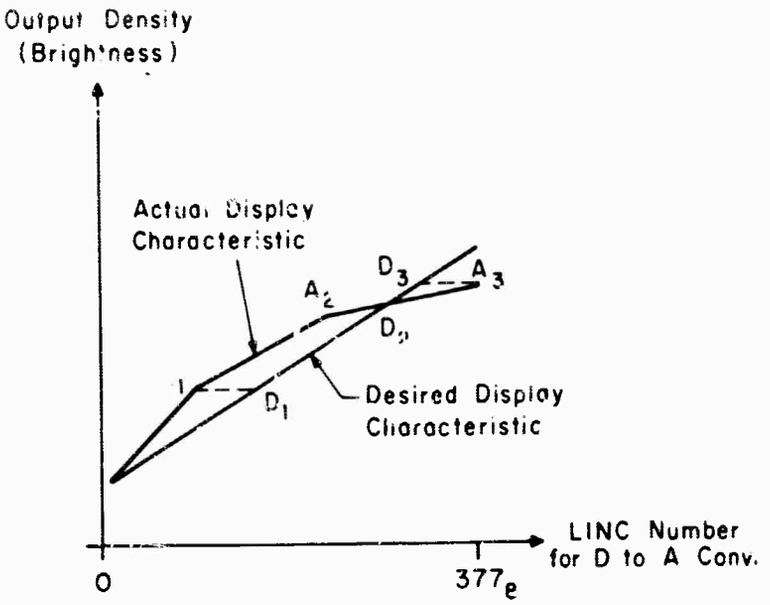

Figure 22. Experimental and Desired Display Characteristics

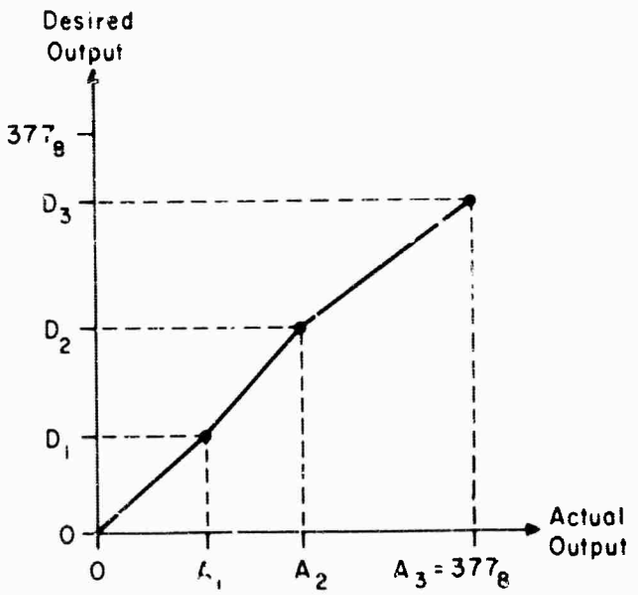

Figure 23. Transfer Relation Between the Experimental and Desired Display Characteristics

of Figure 22. The correction is thus achieved by operating on the actual value with one of the linear functions of Figure 23 thereby obtaining the corresponding ideal output value. The procedure was incorporated into the computer wedge subroutine in which the relationships were established by externally setting the proper coordinates as exhibited in Figure 23 into the program. From the coordinates the slopes were digitally calculated in a manner analogous to the digital contrast enhancement procedure and then employed to compute the equal density steps to be displayed. With the corrected values a density wedge was generated and the densities of each step measured as before. Since the density of the computer wedge was theorized to be in equal steps, the logarithmic voltages representing the densities were plotted against equal LINC number increments as is shown in Figure 24. Also notice that plus and minus ten percent error brackets have been used to account for the nonuniformity of the film and scope. These LINC numbers, N_c, are the actual ones which were digitally processed by the correction subroutine. The resulting curve is a large improvement over the actual curve and one that can be approximated with a straight line as Figure 24 demonstrates. The experimental curve is normally within five to ten percent of the theoretical. The factors which attribute to the discrepancy between the expected and experimental curves are presumed to be the nonuniformity in display brightness, uneven film development and the slight drift in the oscilloscope's intensity.

The Intensity Modulation subroutine is a combination of the computer density wedge's intensifying and the scan's position indexing as indicated by the flow chart of Figure 25. The rectification of the display's nonlinearity characteristic is also programmed into the

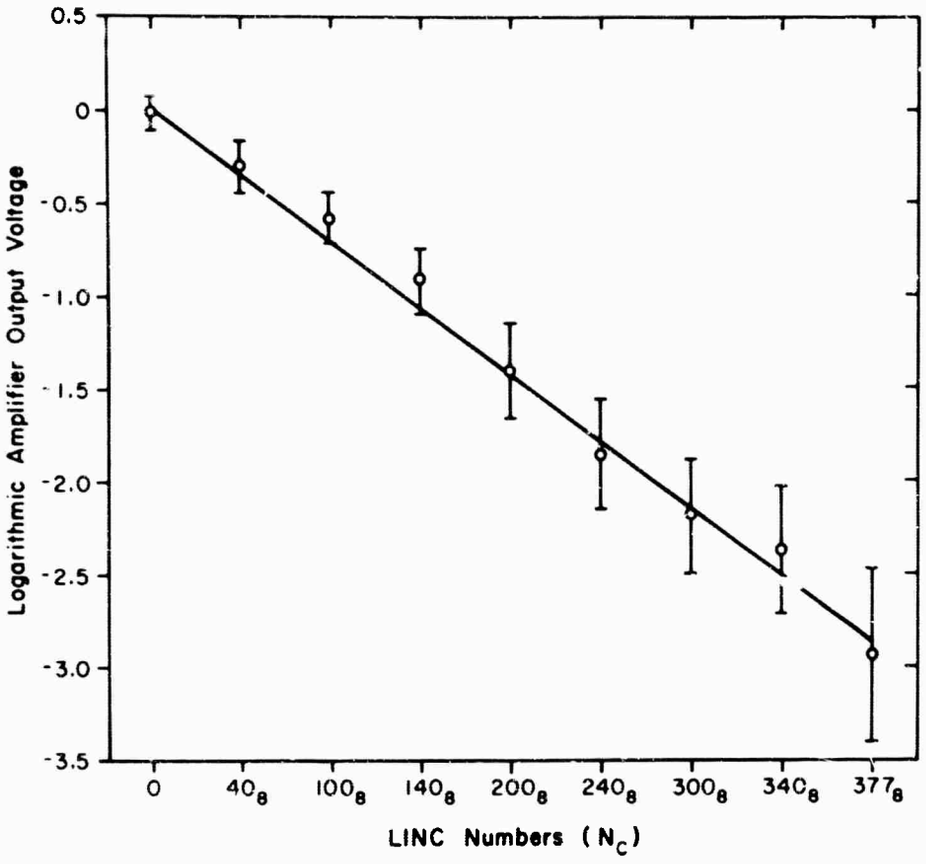

Figure 24 Digitally Corrected Display Characteristic

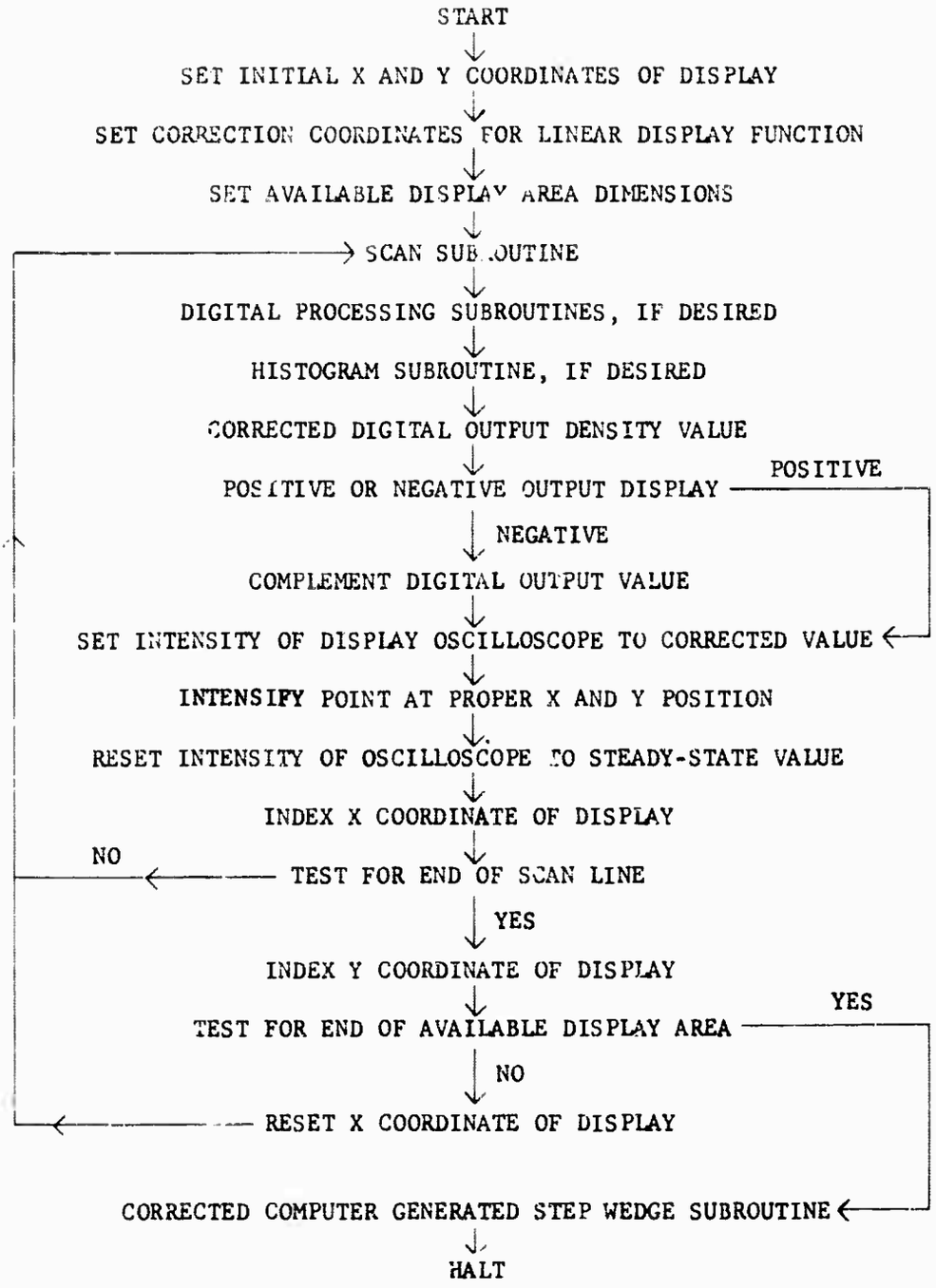

Figure 25. Flow Chart for Intensity Modulation Procedure

display subroutine by means of the correction coordinates as discussed above. Furthermore, a positive or negative output display can be attained by simply complementing the digital value for setting the oscilloscope's intensity as shown in the flow chart. This option is advantageous in certain cases where information not apparent in one perspective becomes more predominant in the other, only because the human observer is more accustomed to viewing it in one and not the other. A good example of this is the picture of a person which is easily recognized in a positive but not a negative as Figure 26 illustrates. Both prints of Figure 26 were produced by scanning the same input transparency of George Washington, but in one the display density was complemented.

After completing a scan, the computer generated wedge is recorded on the film. With the wedge, the density range and the exposure of the output picture can be evaluated by the human operator. Moreover, a decision can be made as to what adjustments are necessary in the display equipment, if any, to optimize the output picture. Most pictures presented have this calibration wedge displayed at the bottom.

In comparing the two different types of multilevel displays, the intensity modulation method is far superior to the dot matrix as a result of the following: (1) increased speed; (2) fewer instructions; (3) a larger display field; (4) finer density quantization; and (5) a wider density range. The last three factors are obvious if one compares the pictures of Figures 19 and 26. Another advantageous factor is that the densities produced by modulating the z-axis are experimentally measureable whereas the dot matrix densities are estimated by a comparison

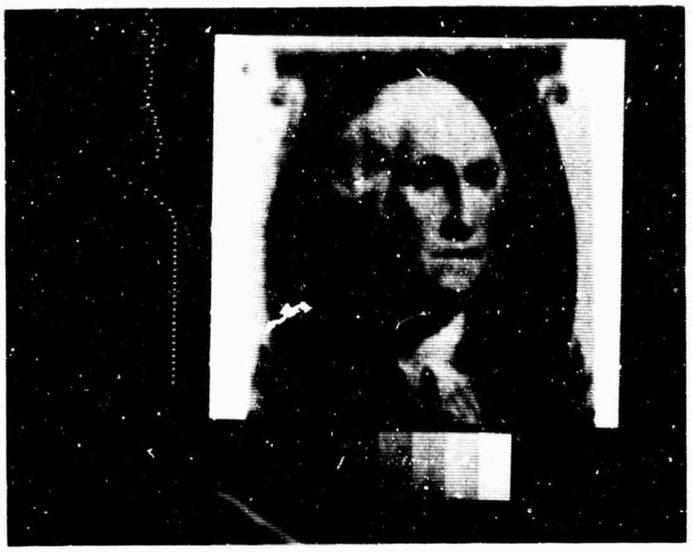

Figure 26. Examples of Positive and Negative Pictures Processed by Intensity Modulation

procedure with the human eye. But the dot matrix enables the operator to view each line of the display as it is produced on the storage oscilloscope. Therefore, digital and analog parameters can be manipulated and the results immediately evaluated instead of having to wait for an entire picture to be processed.

4. CONTRAST ENHANCEMENT AS A MEANS OF RECLAIMING PICTURE INFORMATION

In most transparencies, especially radiographs, much information prevails in regions of relatively low contrast and consequently may be overlooked in an analysis. One possible method to improve these photographs would be to increase the contrast of the picture hopefully revealing recondite detail. If the input contrast were enhanced over the entire output density range, then the maximum degree of enhancement is prescribed by the output density range. Furthermore, by exceeding this limitation some parts of the image become saturated and information is destroyed. Normally, poor contrast does not exist throughout the input image's density spectrum; hence, a more feasible procedure is to enhance the contrast in preferred density regions. Such a process should comprise means of regulating the density range of operation and the magnitude of the contrast enhancement. This chapter will investigate contrast ennancement as a means for recovering picture information. The computer program implementing contrast enhancement, the derivation of a mathematical model representing the system's performance, and quantitative data demonstrating the capabilities of the system will be presented.

4.1 DESCRIPTION OF THE ENHANCEMENT PROCESS

Rather than digitally augmenting the contrast, it is possible to produce contrast enhancement with only an analog process. The method has been illustrated in Figure 27 which shows that almost any degree of contrast enhancement can be procured. The normal curve of Figure 27 depicts the fact that the input contrast is identical to the output contrast which happens only when the input and output densities extend

over equal density increments. The other two curves of Figure 27 exhibit contrast enhancement and compression. By varying the offset and gain controls of the preprocessing circuitry and the output density range, any form of the three representative curves of Figure 27 can be employed. However, several disadvantages exist with linear analog contrast enhancement, specifically: (1) a narrow input density range for high contrast; (2) constant contrast enhancement throughout the input density span; and (3) the offset and gain preprocessing circuit parameters must be readjusted each time the output contrast is to be varied. With a small input density spectrum, only a segment of the input appears on the output picture making it rather difficult to correlate the enhanced information with the remainder of the picture. In most cases, several density regions of the input image require various degrees of contrast enhancement. This implies that a series of output pictures must be produced, each with different circuit parameter settings. Finally, good reproducibility of analog enhancement is almost impossible to attain since it is extremely difficult to reset analog parameters to the exact values. A better procedure involves a computer program in conjunction with the analog enhancement where the above disadvantages are minimized.

Before explaining the contrast enhancement program, the sampling technique of input densities will be briefly reviewed. When the input transparency is sampled by the LINC through the analog to digital converter, an octal number between $+177_8$ and -177_8 denoting a density is read into the computer for processing. Usually, the preprocessing entails the logarithmic amplifier, thus the octal numbers are linearly proportional to the input film's density. The digital contrast

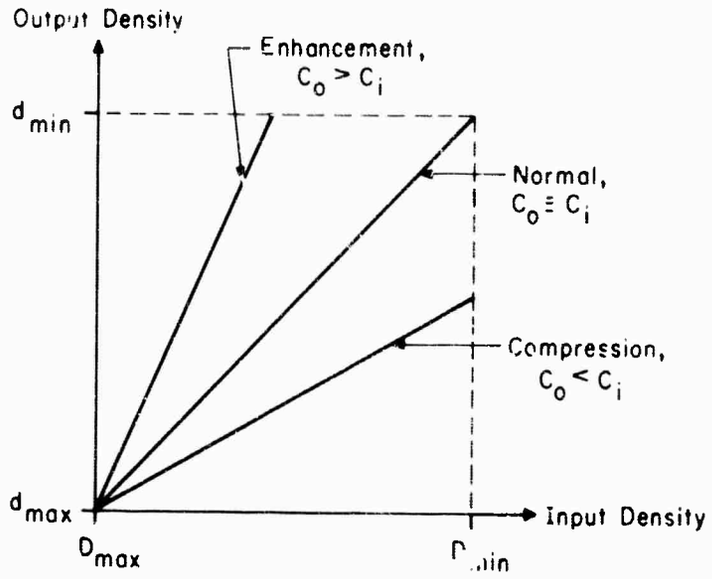

Figure 27. Analog Contrast Enhancement Possibilities

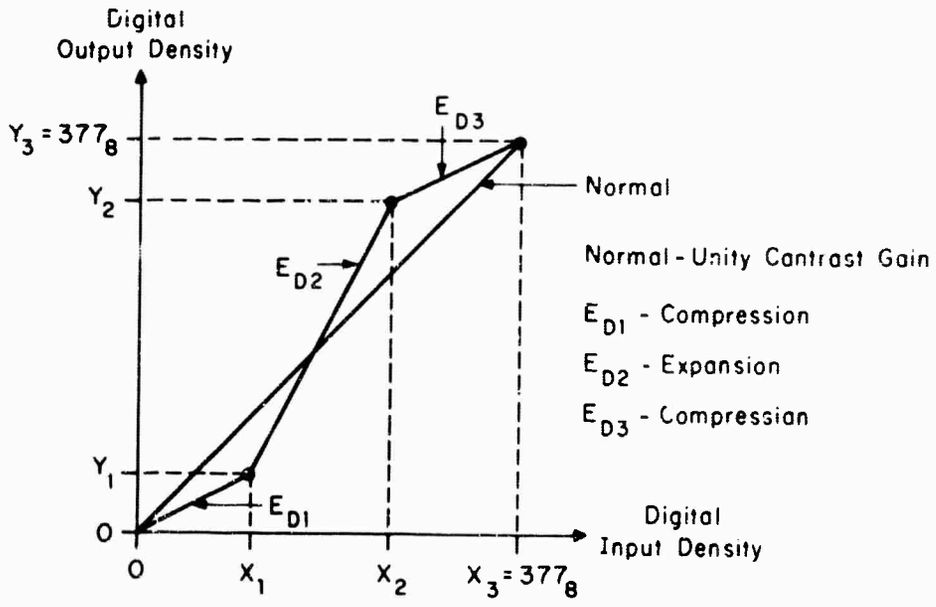

Figure 28. Typical Digital Contrast Enhancement Function

enhancement can then be applied directly to the numbers. If any analog contrast enhancement has occurred, then the digital process operates on the result providing further enhancement if requested. To facilitate the computing and programming of the digital contrast enhancement, the above octal numbers are offset by 200_8 in order that the lowest input density is designated by 377_8 and the highest by zero.

The principal functions incorporated into the enhancement program are examplified in Figure 28 by the discontinuous but connecting straight lines. These lines relate the input density to the output density, and the curves of Figure 28 depict contrast compression and expansion are possible over any input density ranges. The normal line describes unity digital contrast enhancement meaning that the digital input contrast equals the output contrast.

A flow chart describing the operations of the contrast enhancement program is presented in Figure 29. The present program partitions the input density into defined sections, each receiving a specified type of contrast enhancement depending on the discretion of the operator. By reading into the computer the X (input density) and Y (output density) coordinates of the desired slopes and the density span of each slope, then the program proceeds to calculate the exact slopes. The value of the slopes must be between 0.001_8 and 30_8 which is sufficient enhancement as will be demonstrated when the mathematics of the system are analyzed. In computing the slopes from the coordinates, the first slope is assumed to pass through the origin, (0,0) on Figure 28. Also, the last X coordinate must be equal to 377_8 for the entire input density spectrum to be included; and the last Y coordinate

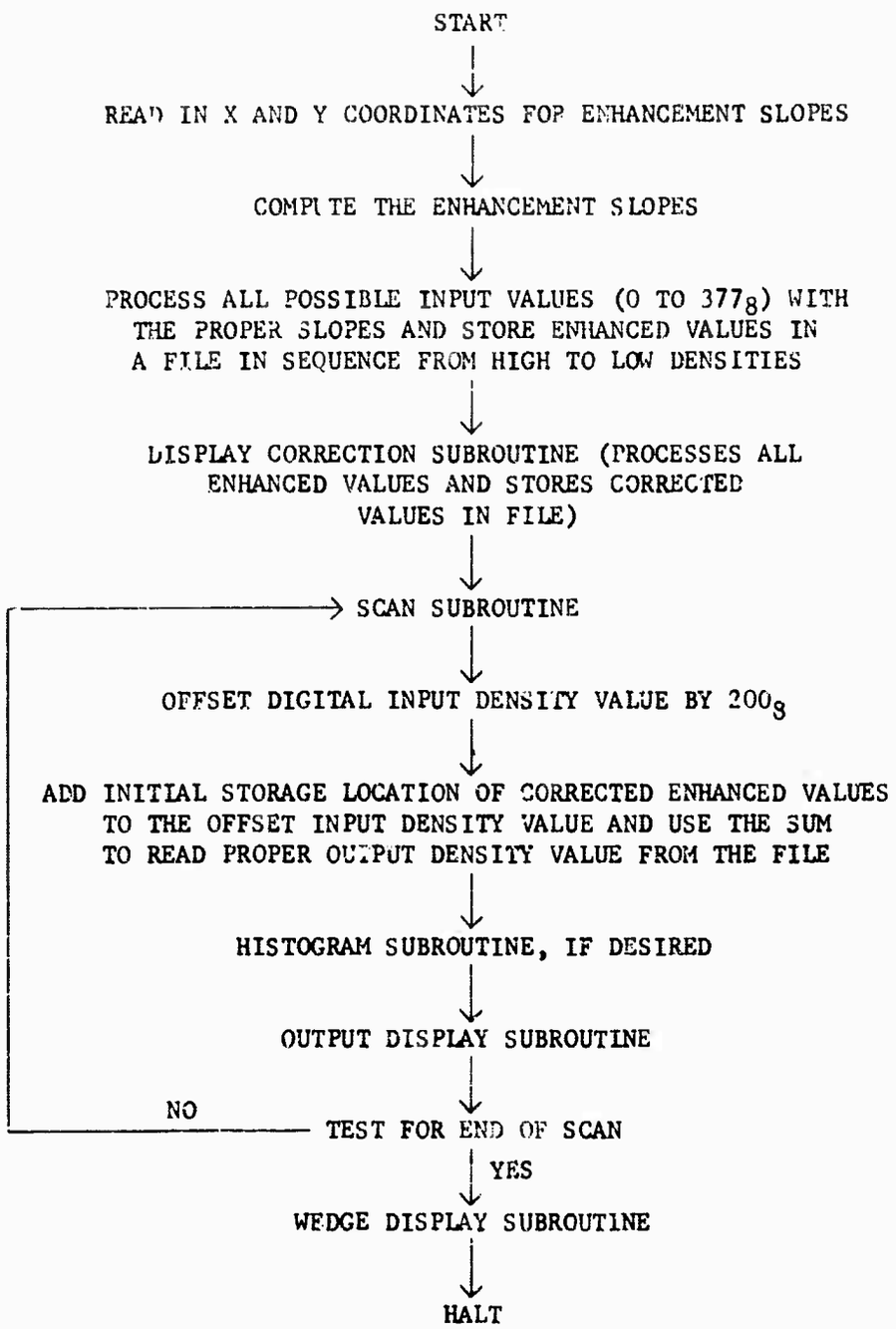

Figure 29. Flow Chart for Contrast Enhancement Subroutine

cannot exceed but may be less than 377_8, since above this number has no meaning as far as output densities are concerned. The maximum number of enhancement slopes is five which has adequately processed most transparencies thus far considered; however, should the need arise the number can easily be augmented. With this arrangement contrast expansion or compression can be performed on any input density range if the proper X and Y coordinates are specified; and to vary the slopes one only resets the coordinates.

Upon calculating the slopes, all the possible digital input values from zero to 377_8 are processed with the proper enhancement curve. The enhanced values, output densities, are stored in a file in the sequence of high to low densities. This greatly reduces the total processing time in that most input values occur many times during a scan, and for each value the file is merely consulted for a corresponding output density instead of repeating a lengthy computation.

One limitation of the contrast enhancement technique is that in order to augment the contrast in one section of the input density range, the contrast must often be diminished in another. This is caused by the fact that the output film has a restricted density range. By decreasing the contrast, important information can be suppressed; therefore, one must carefully select the slopes which yield the optimum contrast in one region and yet retain as much contrast as possible in the others.

Besides the flexible method for assigning the contrast enhancement, the subroutine itself can be easily merged into any display subroutine where it is important to control contrast. An example where the subroutine has been successfully operated will be described in Chapter 5

with the subtraction program. The same basic subroutine, which calculates the slopes and processes all the possible input values, is also employed in computing the corrected output density values. The procedure is similar except that coordinates representing the actual and desired digital values are read into the subroutine.

4.2 ANALYSIS OF THE MATHEMATICAL MODEL

For this image processing system a mathematical model of the overall system's operations and characteristics was defined. Ideally, equations relating the output film density in terms of the density of the input transparency would be instrumental in better understanding the system. The equations would also provide a fine control over the analog and digital processes and the display of the system; therefore, a mathematical derivation of the system's operations will be presented.

4.2.1 Introduction

The basic functions of the system to be considered in the derivation are separated into the following: (1) image dissector camera; (2) analog processing, (3) digital processing; and (4) display. These units are illustrated in the series block diagram of Figure 30. The general form of the equations was assumed in order that several different processes could be considered without going through separate derivations for each.

Each equation describing a particular operation or characteristic is shown as a transfer function of only one variable, namely the output of the preceeding process, to simplify the analysis. The equations characterizing the functions designated in Figure 30 are respectively:

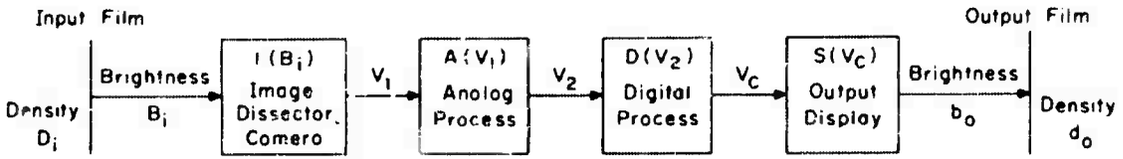

Figure 30. Mathematical Model of the System

$$V_1 = I\ (B_i) \qquad \text{Equation (6)}$$

where B_i is the input brightness of the input image,

$$V_2 = A\ (V_1) \qquad \text{Equation (7)}$$

$$V_c = D\ (V_2) \qquad \text{Equation (8)}$$

$$b_o = S\ (V_c) \qquad \text{Equation (9)}$$

where b_o is the output brightness of the output image. Therefore, the general form of the system's equation becomes

$$b_o = S\ (D\ (A\ (I\ (B_i)))) \qquad \text{Equation (10)}$$

where Equations (6), (7), (8), and (9) have been combined. An equation for brightness in terms of density is expressed as

$$B = B_R 10^{-D} \qquad \text{Equation (11)}$$

where D is the density and B_R is a constant. More specifically, the equations defining the input and output brightness are

$$B_i = B_1 10^{-D_i} \qquad \text{Equation (12)}$$

$$b_o = b_1 10^{-d_o} \qquad \text{Equation (13)}$$

where D_i and d_o are densities on the input and output films respectively. Furthermore, the contrast, C, of an optical image is defined as

$$C = \frac{\text{Image Brightness - Background Brightness}}{\text{Background Brightness}} \qquad \text{Equation (14)}$$

Finally, the contrast gain of the system infers

$$C_g = \text{contrast gain} = \frac{\text{Output Contrast}}{\text{Input Contrast}} \qquad \text{Equation (15)}$$

$$C_g = \frac{C_o}{C_i} \qquad \text{Equation (16)}$$

where C_o is the output contrast and C_i the input contrast. This concludes the initial setup of the mathematical model which will be used in the following analyses.

4.3.2 Analysis of a Simple Linear System

For the first derivation a completely linear image processing system was assumed, hence, each of the four transfer functions reduces to linear relationships. Thus, the form of Equation (10) for such a system can be surmised to be

$$b_o = K + K_o B_i \qquad \text{Equation (17)}$$

where K_o and K are constants. Expanding Equation (17) by substituting Equations (12) and (13), setting the bias, K, equal to zero, taking the logarithm of both sides and simplifying, the resulting expression is

$$d_o = K_2 + K_1 D_i \qquad \text{Equation (18)}$$

where K_1 equals one and K_2 is a constant.

In order to evaluate the values of K_1 and K_2 the boundary conditions concerning the input density and output density ranges must be considered. Although the image dissector camera's density range is rather wide, only a portion of it is digitized by the LINC depending on the setting of the preprocessing circuit parameters. The input density spectrum is established with a Kodak Density Step Wedge whereby a particular maximum and minimum input density, D_{max} and D_{min}, are set

into the analog preprocessing unit. The output density range is restricted by either the oscilloscope or the output film, depending on the type of film employed. For the transparent film, the limiting factor is the intensity of the oscilloscope; however, for the print film the output density range is constrained by the film capabilities. In either case, the maximum and minimum output densities are referred to as d_{max} and d_{min}, respectively. In computing the constants, it is assumed for the minimum input density that the minimum output density is recorded on the film and similarly for the maximum input density. Solving for K_1 and K_2 by inserting these boundary conditions results in Equations (19) and (20)

$$K_1 = \frac{d_{min} - d_{max}}{D_{min} - D_{max}} \qquad \text{Equation (19)}$$

$$K_2 = \frac{d_{max}D_{min} - d_{min}D_{max}}{D_{min} - D_{max}} \qquad \text{Equation (20)}$$

which are only valid for the bias, K, equal to zero.

The input contrast may be expressed as shown in Equation (21)

$$C_i = \text{input contrast} = \frac{B_I - B_B}{B_B} \qquad \text{Equation (21)}$$

where B_I is the brightness of the image and B_B is the brightness of the background. Using Equation (17) where the output brightness is directly proportional to the input brightness, then the output contrast becomes

$$C_o = \text{output contrast} = \frac{B_I - B_B}{B_B + K/K_1} \qquad \text{Equation (22)}$$

Consequently, the contrast gain for the linear system equals

$$C_g = \frac{C_o}{C_i} = \frac{B_B}{B_B + K/K_o} \qquad \text{Equation (23)}$$

Equation (23) reveals that contrast enhancement, C_g greater than one, is possible for the linear system only when the parameters are adjusted such that the K/K_o is negative. For the case of K/K_o greater than zero the contrast enhancement is less than one; therefore, the contrast of the output image is suppressed. If K/K_o should equal zero which can be accomplished by setting the bias, K, equal to zero, then the contrast gain equals unity.

$$C_g = \frac{C_o}{C_i} = 1 \qquad \text{Equation (24)}$$

In this situation the input density does not necessarily have to be equivalent to the output density for the equation to be valid. The final expressions representing the linear model are rather obvious; however, the reasoning leading up to them parallels that which will be used to obtain the equations for a more complex system.

4.2.3 Analysis of the Experimental System

The configuration of the actual image processing system which was constructed and tested in this research is the subject of the next derivation. The same procedure outlined in developing the linear system's equations will be followed again. However, each of the four transfer functions indicating different operations of the system will have to be dealt with individually and then combined.

The image dissector camera, as was experimentally verified, is a linear device with respect to input density. Therefore, Equation (6)

becomes

$$V_1 = I(B_i) = I_1 B_i \qquad \text{Equation (25)}$$

where I_1 is a constant.

Two different analog functions, linear and logarithmic, are available to process the image dissector camera's voltage. The derived results of both processes has been performed, but only the derivation with the logarithmic amplifier is presented in detail since the two are somewhat similar.

The purpose of the logarithmic amplifier is to provide the digital processes with a value that is linearly proportional to the input film's density. Clearly, the logarithmic amplifier is mathematically represented by Equation (26)

$$V_2 = A(V_1) = A_1 \log V_1 + A_2 \qquad \text{Equation (26)}$$

where A_1 and A_2 are constants. By substituting Equation (25) into Equation (26) and inserting the definition for input brightness, Equation (12), one arrives, after simplifying, at Equation (27)

$$V_2 = K_3 + K_4 D_i \qquad \text{Equation (27)}$$

where K_3 and K_4 are both constants. Thus, the input voltage to the analog to digital converter is linear with respect to input density which facilitates programming any digital operations.

The computer enables the operator to digitally amplify or attenuate the digital representation of the input density. Both amplification and attenuation can be <u>linearly</u> achieved on the same input film but over different density ranges contingent on where more contrast is required.

The operator controls the degree of contrast enhancement as well as the density spectrum where the enhancing is to be executed, which was demonstrated in Section 4.1.

Therefore, the LINC number (N_c) which is supplied to the digital display correction subroutine is linearly related to V_2 by Equation (28)

$$\bar{N}_c = D(\bar{N}_c) = K_6 + K_5 V_2 \qquad \text{Equation (28)}$$

where K_5 and K_6 are constants, and $\bar{N}_c$ is the decimal equivalent of N_c. For each input density segment where the contrast enhancement differs, a new set of values for K_5 and K_6 prevail denoting the degree of digital contrast enhancement in that range. Theoretically, K_5 may have a value anywhere between zero and infinity; however, the program limitations are between 0.001_8 and 30_8 which will be shown to be sufficient. Expanding Equation (28) by substituting Equation (27) yields

$$\bar{N}_c = K_6 + K_5 K_3 + K_5 K_4 D_i \qquad \text{Equation (29)}$$

which describes the LINC number for the output density before the digital display correction subroutine in terms of the input film density.

The last function to be determined includes the output display characteristics and operations. A relationship between N_c and the output film density had to be evaluated. In order to obtain the relationship, several experiments were performed whereby the z-axis voltage change was recorded onto Polaroid transparent film. The density of the film spans from a density of 0.05 to 2.40; however, the linearity of the film does not extend over the entire range as mentioned earlier (22). The most linear part of the film exists over the density of 0.55 to 1.55; hence, the display relationship that is discovered should also include the film's nonlinearity characteristic.

After exposing the digitally corrected step wedge on transparent film the logarithmic amplifier was established to cover the densities from 0.05 to 2.25 with the Kodak Density Step Wedge. n, the density steps of the comp ter wedge were measured with the image dissector camera by comparing the output voltages of the logarithmic amplifier to the curve of the Kodak Wedge. The digital display correction subroutine processes LINC numbers (N_c) in equal intervals of 40_8 for the computer generated wedge. The densities have been plotted against the related LINC numbers as shown in Figure 31. Each measured density is indicated with plus and minus ten percent error brackets which compensate for uneven development and graininess of the film together with the scope's phospher variation. From the curve the general equation of the display, including the digital display correction routine, becomes

$$S_2(\bar{N}_c) = S_2 10^{K_7\bar{N}_c} = b_1 10^{-d_o} \qquad \text{Equation (30)}$$

where K_7 and S_2 are constants.

If Equation (29) is substituted into Equation (30), the result is Equation (31)

$$b_o = K_8\ 10^{K_5K_9 + K_5K_{10}D_i + K_7K_6} \qquad \text{Equation (31)}$$

where the new constants are K_8, K_9, and K_{10}. Proceeding one step further by inserting for b_o, Equation (13), and reducing yields Equation (32)

$$d_o = K_{11} + K_{12}K_5D_i \qquad \text{Equation (32)}$$

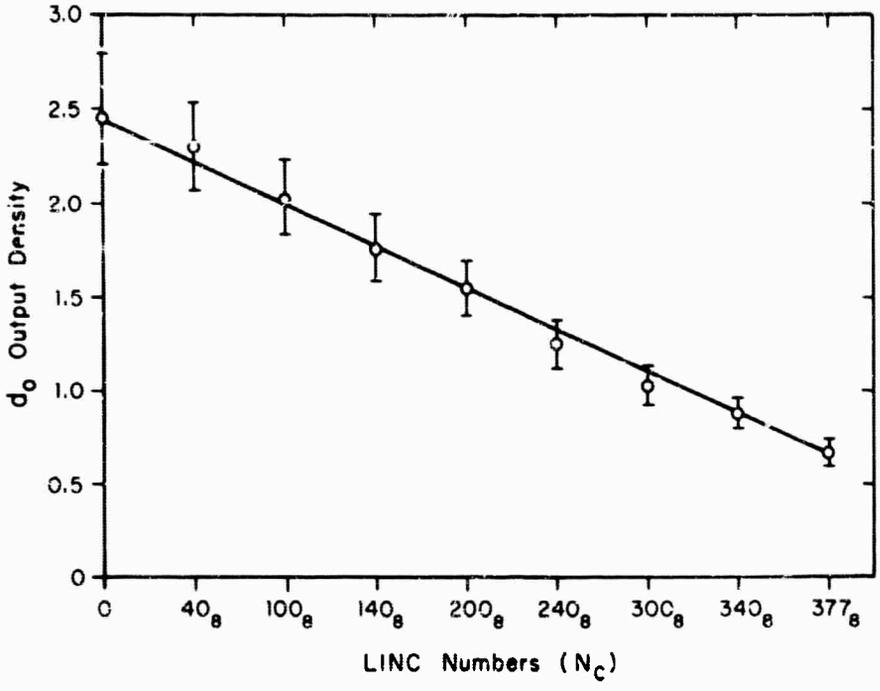

Figure 31. Linearity Test of Computer Generated Densities

This is the desired relationship explicitly defining the output density in terms of the input density.

For the case where no digital process occurs, K_5 equals one, and Equation (32) simplifies to

$$d_o = K_{11} + K_{12}D_i \qquad \text{Equation (33)}$$

Equation (33) is identical to Equation (18) which was previously derived for the completely linear system. The constants, K_{11} and K_{12} of Equation (33), are the same as those in Equation (20) and Equation (19) respectively. However, when evaluating the constants of Equation (32) the boundary conditions established by the digital contrast enhancement process must be examined. For each slope in the digital process a different set of constraints exist as will be demonstrated. To assist in explaining exactly how the constants are evaluated, a typical contrast enhancement curve is manifested in Figure 32. The maximum and minimum input densities are translated into LINC values (decimal equivalent) of zero and 256 respectively, and for densities between these a linear function, Equation (34),

$$D_i = D_{max} + \frac{X(D_{min} - D_{max})}{256} \qquad \text{Equation (34)}$$

relates the input density to X, its LINC equivalent. A similar relationship for the output densities and the corresponding LINC value Y, is

$$d_i = d_{max} + \frac{Y(d_{min} - d_{max})}{256} \qquad \text{Equation (35)}$$

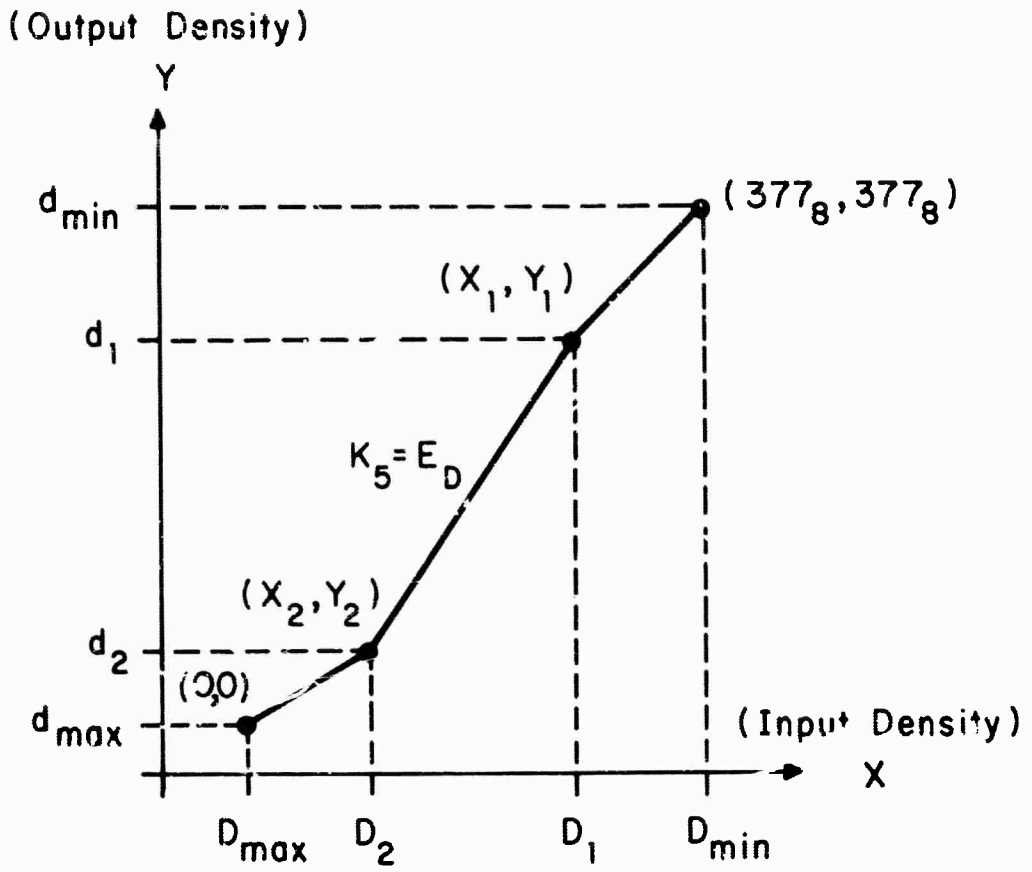

Figure 32. Typical Contrast Enhancement Curves Relating Input and Output Densities to Digital Values

where d_{max} and d_{min} are the displayed maximum and minimum densities. If the coordinates of the slope are inserted into these equations, then the boundary conditions for a particular slope become

$$D_1 = D_{max} + \frac{X_1(D_{min} - D_{max})}{256} \qquad \text{Equation (36)}$$

$$D_2 = D_{max} + \frac{X_2(D_{min} - D_{max})}{256} \qquad \text{Equation (37)}$$

$$d_1 = d_{max} + \frac{Y_1(d_{min} - d_{max})}{256} \qquad \text{Equation (38)}$$

$$d_2 = d_{max} + \frac{Y_2(d_{min} - d_{max})}{256} \qquad \text{Equation (39)}$$

Therefore, for an input density D_1, the corresponding output density is d_1, and likewise for an input density D_2, the output density is d_2. Substituting these expressions into Equation (32) and solving for K_{11} and K_{12} yields

$$K_{11} = \frac{d_1D_2 - d_2D_1}{D_2 - D_1} \qquad \text{Equation (40)}$$

$$K_{12} = \frac{d_2 - d_1}{(D_2 - D_1)K_5} \qquad \text{Equation (41)}$$

where K_5 represents the digital contrast enhancement as shown in Figure 32. With these constants and Equation (32), the output density can be calculated for any particular input density which will be experimentally verified in the next section.

If Equations (12) and (13) are solved for the densities and then substituted into Equation (32), the results may be reduced to

$$b_o = K_{13} b_i^{E} \qquad \text{Equation (42)}$$

where $K_{13} = 10^{-K_{11} b_1 (B_1)^{-K_{12}K_5}}$, $E = K_{12}K_5 = E_A E_D$ which will be referred to as the contrast constant. E_A represents the analog enhancement constant; and E_D, the digital enhancement constant. Introducing Equation (2) into Equation (14) and simplifying, the output contrast becomes

$$C_o = \left(\frac{B_I}{B_B} \right)^{E} - 1 \qquad \text{Equation (43)}$$

or expanding with Equation (12)

$$C_o = 10^{(D_B - D_I)E} - 1 \qquad \text{Equation (44)}$$

The input contrast is defined by Equation (21) which when put in terms of density is

$$C_i = 10^{(D_B - D_I)} - 1 \qquad \text{Equation (45)}$$

With Equations (44) and (45) the contrast gain, C_g, may be expressed as the ratio of output to input contrast as Equation (46) shows

$$C_g = \frac{C_o}{C_i} = \frac{10^{(D_B - D_I)E} - 1}{10^{(D_B - D_I)} - 1} \qquad \text{Equation (46)}$$

To closely examine the case where $(D_B - D_I)$ is small, an exponential series of the form

$$a^x = 1 + x \log_e a + \ldots. \qquad \text{Equation (47)}$$

is employed to expand Equation (44) into the following,

$$C_o = E(D_B - D_I)\log_e 10 \qquad \text{Equation (48)}$$

Equation (48) indicates that the output contrast is linearly related to the contrast constant for small input density differences. A similar substitution into the contrast gain expression yields

$$C_g = E \qquad \text{Equation (49)}$$

which is verified for the special case, $(D_B - D_I)$ equals zero, by applying L'Hopital's rule to Equation (46).

A family of curves representing Equation (46) with various values for the contrast constant, E, is illustrated in Figures 33 and 34. For E equal to one, the output contrast equals the input contrast; however, for E greater than one the contrast gain follows an exponential function in which the contrast gain increases with the input density difference.

Also plotted in Figure 33 is a series of curves designating the maximum contrast gain attainable due to the limitations of the film and the display. The output contrast may be expressed in an equation similar to Equation (45) which redefines the contrast gain as

$$C_g = \frac{C_o}{C_i} = \frac{10^{(d_B - d_I)} - 1}{10^{(D_B - D_I)} - 1} \qquad \text{Equation (50)}$$

To compute each of the contrast limitation curves, a particular maximum output density range, $d_{max} - d_{min} = \Delta d_{max}$, is specified by the film and display capabilities and assumed to be totally exploited for each possible input density range, $D_1 - D_2$, as exemplified by Equation (51),

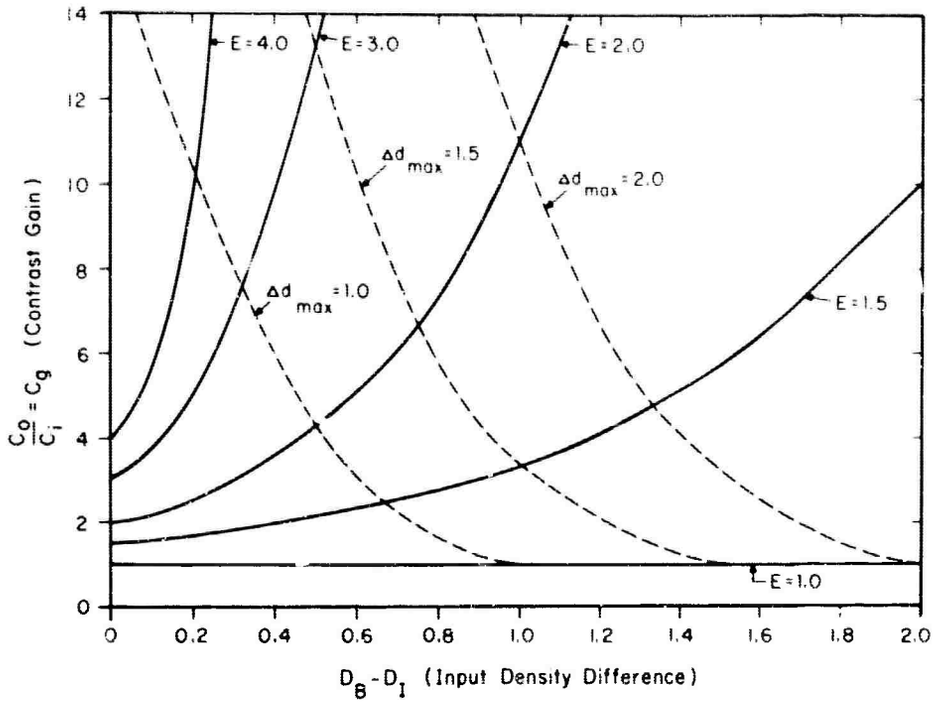

Figure 33. Influence of the Contrast Constant, E, and Density Difference on Contrast Gain (for E ≥ 1)

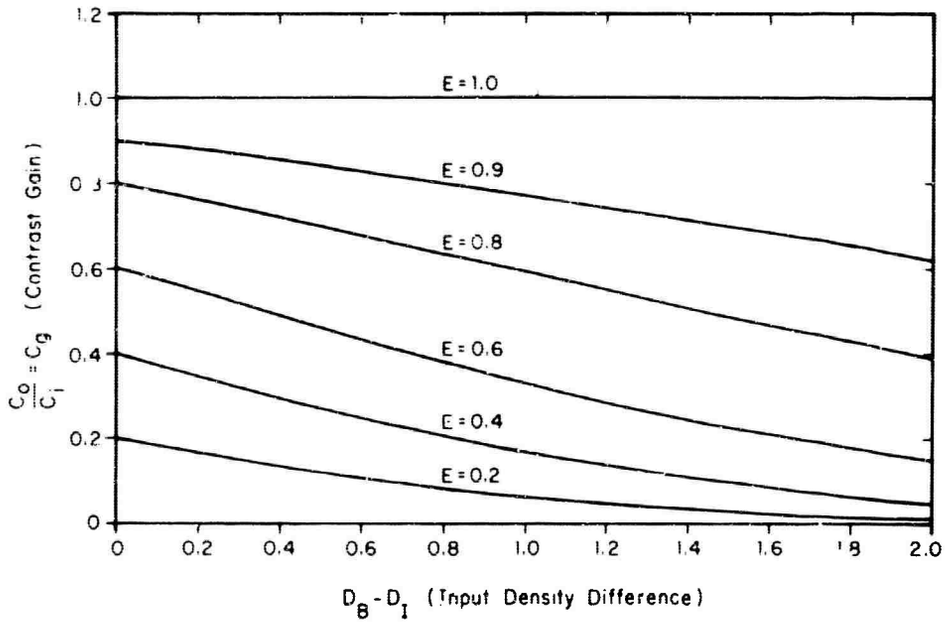

Figure 34. Influence of the Contrast Constant, E, and Density Difference on Contrast Gain (for E ≤ 1)

$$C_{g\ max} = \frac{C_{o\ max}}{C_i} = \frac{10^{\Delta d_{max}} - 1}{10^{(D_1 - D_2)} - 1} \qquad \text{Equation (51)}$$

For each output picture only one of these curves is valid which implies that contrast gain above it would be physically impossible to produce. The curves of Figure 34 are for E less than one, hence, the contrast gain is also less than one, which is the case of compression. But the degree of compression is rather gentle when compared to the enhancement curves where E is greater than one. With the curves of Figure 33 and 34 the desired output contrast enhancement can be optimally set for a specific input density difference.

If E_A equals one, which can be realized by properly adjusting the preprocessing circuit parameters such that the input and output densities have the same difference between maximum and minimum densities, then E equals E_D. With this condition satisfied, the output contrast is theoretically ascertained by only the digital slopes. An example of this type of control will be described in the experimental results section together with some quantitative data.

4.3 EXPERIMENTAL RESULTS

The next step is to verify that the above derived equations do indeed represent the operations of the image processing system by applying them to some experimental data. If these equations reasonably predict the output density for a particular input density, then the contrast enhancement required to distinguish between two input densities on the output film can be computed. But differentiating between densities with the human eye entails several psychological factors (12,13,14) which have not been completely explained at the present and are beyond the

scope of this report. Assuming that the psychological factors are mathematically expressible and the minimum amount of contrast between two objects to distinguish them from each other is known, then from the derived equations the optimum contrast can be achieved. In addition, the system's mechanics are easily comprehended with the aid of the equations. The procedure and results for establishing the validity of the equations will be described in this section. Also presented is a series of pictures illustrating the value of digitally processing with contrast enhancement.

4.3.1 Verification of System's Equations with Quantitative Data

The input transparency selected for this investigation was composed of simple geometric figures, labelled A through E, varying in density from approximately 0.10 to 0.90. The density, D_i, of each figure was relatively uniform and therefore could easily be measured with the image dissector camera. In setting up the analog apparatus the logarithmic amplifier was adjusted to include input densities between 0.03 and 1.20, D_{min} and D_{max}, which are shown in Figure 10, where Kodak density steps are plotted against the logarithmic amplifier's output voltage. To facilitate the computations, the digital contrast enhancement, E_D, was set equal to unity and thus Equation (32) simplifies to Equation (33), as was indicated earlier.

The resulting output picture with a linear computer generated wedge was exposed on the transparent film. The densities of the wedge and of the output geometric figures were experimentally measured and recorded. Next, densities of the computer wedge were plotted to determine if a linear wedge had been achieved, and if so, the maximum and minimum output

densities, d_{max} and d_{min}, were acquired by extrapolating the curve as demonstrated in Figure 35.

Now that the input and output boundary conditions have been defined by the curves of Figure 10 and 35a, the constants of Equation (33), K_{11} and K_{12}, can be evaluated according to Equations (19) and (20) respectively, after which Equation (33) becomes

$$d_o = 0.54 + 1.29\ D_i \qquad \text{Equation (52)}$$

With this equation, a theoretical output density can be calculated for any input density within the range of D_{max} and D_{min}. However, instead of measuring the input densities with the usual method, the input histogram subroutine was executed to obtain the dynamic densities. Since each of the geometric figures differed in density, several distinct peaks appeared on the histogram where each represented a particular figure's density. From these peaks the input densities were measured thereby attaining the actual densities sampled by the computer for digital processing and also eliminating any nonuniformity in the light field. The input density values were then substituted into Equation (52) and the predicted output densities, d_o, computed. Table 2 lists the theoretical and experimental output densities for each of the input figures together with a percent of error. The error factor is a function of the definition and may be defined in one of several ways, but one was selected to provide a standard for comparison. The percent of error in Table 2 is defined as the difference between the theoretical and experimental values divided by the theoretical density, and then multiplied by one hundred. The uneven development and graininess of the transparent film have contributed to these errors but an average value

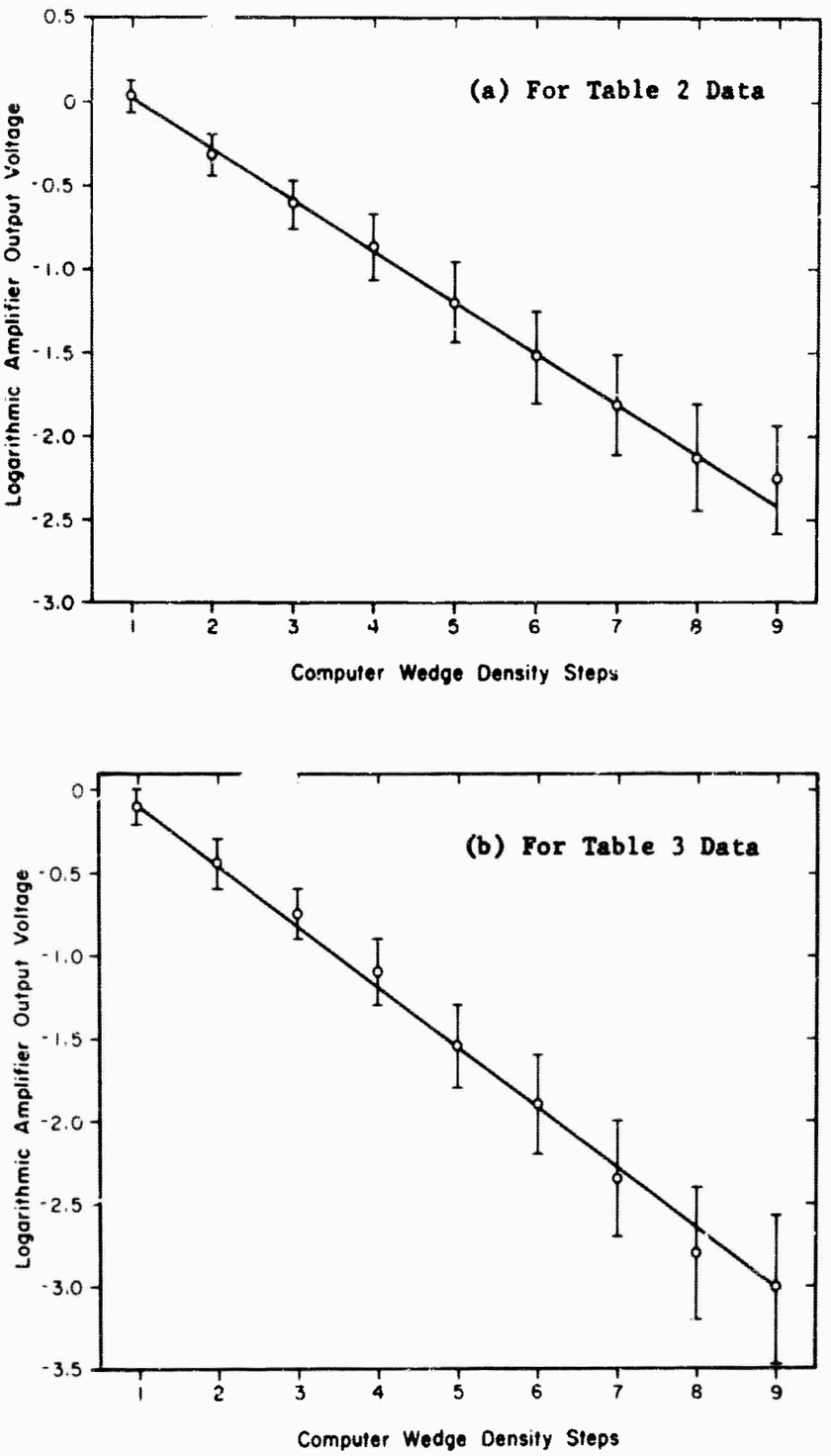

Figure 35. Plot of Computer Generated Density Wedge

Table 2 A Comparison of Experimental and Theoretical Film Densities for Unity Digital Contrast Enhancement

GEOMETRIC FIGURE	INPUT DENSITY (LINC NUMBER)	INPUT DENSITY D_i	OUTPUT DENSITY		PERCENT ERROR
			EXPERIMENTAL d_c	THEORETICAL d_o	
A	345_8	0.16	0.83	0.75	-10.7
B	315_8	0.27	0.94	0.89	-5.7
C	213_8	0.57	1.30	1.27	-2.3
D	160_8	0.69	1.48	1.44	-2.8
E	103_8	0.90	1.80	1.70	-5.9

Table 3 A Comparison of Experimental and Theoretical Film Densities for the Digital Contrast Enhancement Shown in Figure 36

GEOMETRIC FIGURE	INPUT DENSITY (LINC NUMBER)	INPUT DENSITY D_i	OUTPUT DENSITY		PERCENT ERROR
			EXPERIMENTAL d_o	THEORETICAL d_o	
A	345_8	0.16	0.74	0.78	5.1
B	315_8	0.27	0.97	1.06	8.5
C	213_8	0.57	1.70	1.89	10.0
D	160_8	0.69	1.97	2.06	4.4
E	103_8	0.90	2.36	2.33	-1.3

of density was obtained from repeated measurement to minimize these objectionable features. Moreover, the nonuniformity of the scope was checked and the most uniform region was then utilized.

Further examination entailed scanning the same transparent film only this time with digital contrast enhancement processing. The slopes and coordinates implementing the enhancement are designated in Figure 36. Using the LINC numbers of Table 2 which are equivalent to the input densities it can be determined that densities of geometric figures A and B are processed with a slope of 1.55_8, figure C by 2.0_8 and figures D and C by 1.0_8. These slopes were selected for the purpose of exploiting the entire output density range with the input density range of the figures thus increasing the density differences between some of the objects. Since no adjustments were made concerning the analog parameters, the curve representing the input density spectrum of the previous scan, Figure 10, remains valid for the present scan.

As before, the output densities of the geometric figures and the computer wedge were measured. The wedge densities are plotted in Figure 35b and the experimental output densities of the figures are recorded in Table 3. With the input histogram subroutine the input densities are remeasured to insure against any analog drift occurring between the two scans and are designated in Table 3.

The boundary conditions of the system are determined by the input and output curves of Figures 10 and 35b respectively, but because of the digital contrast enhancement, Equation (32) must be employed in calculating the theoretical output densities; therefore, another set of boundary conditions imposed by the slopes will have to be considered in evaluating the constants K_{11} and K_{12}. These constants are defined by

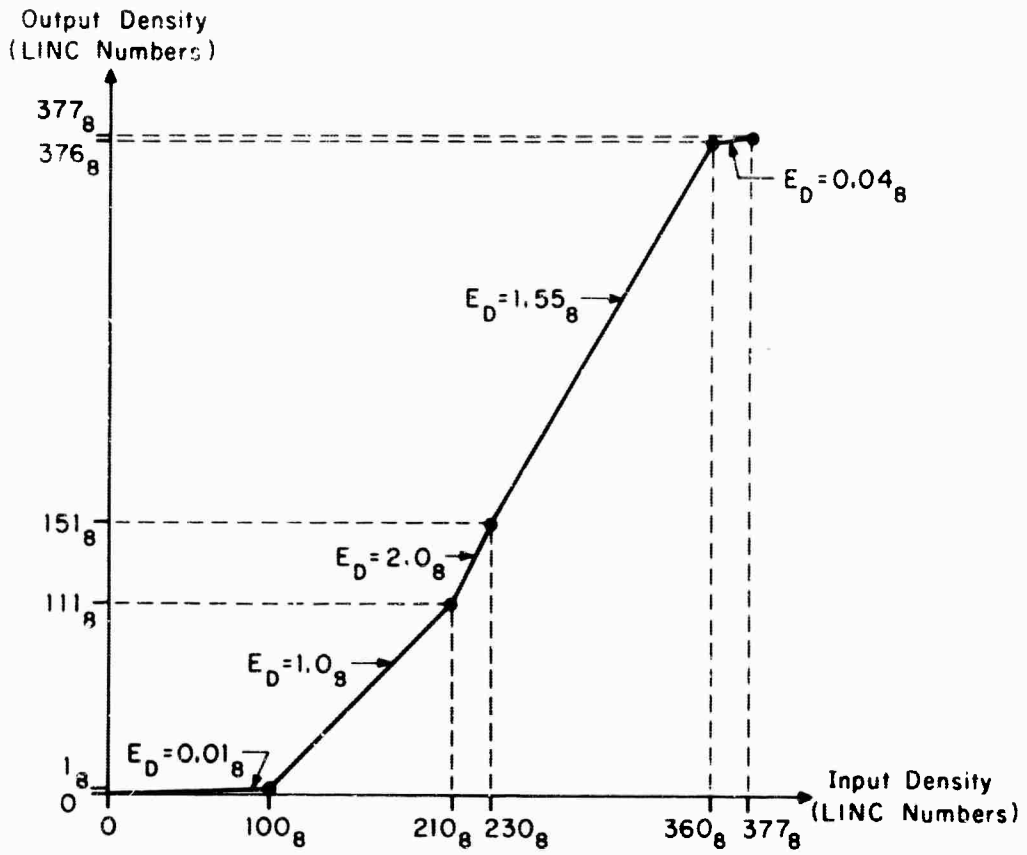

Figure 36. Digital Contrast Enhancement Curves

Equations (40) and (41) and when computed and substituted into Equation (39) yield the following three equations each of which characterizes a particular segment of the input density range.

$$d_o = 1.13 + 1.31\ D_i \qquad 0.70 \leq D_i \leq 0.91$$

$$d_o = 0.10 + 3.14\ D_i \qquad 0.11 \leq D_i \leq 0.59 \qquad \text{Equation (53)}$$

$$d_o = 0.38 + 2.53\ D_i \qquad 0.12 \leq D_i \leq 0.31$$

From these equations the theoretical output densities were calculated for each of the geometric figures with the results listed in Table 3. Note how the higher contrast gain for Figures A, B and C produces a larger density difference (contrast) between pairs of these figures in Table 3 than is produced by the corresponding pairs in Table 2. In addition, the system of Table 3 achieves the objective of utilizing more of the output density range of the film.

Considering the uneven film development and other sources of experimental error, it appears that the theoretical density relations for the image processing system are varified by the experimental results of Tables 2 and 3.

4.3.2 Some Typical Processed Pictures

To illustrate exactly how one might effectively employ the digital process of contrast enhancement, a brief discussion with some quantitative data will be presented. An angiogram, which is a radiograph of blood vessels in which an opaque material has been injected, was selected for the experiment because of the attractive feature that much information exists in regions where the contrast is comparatively low. With contrast

enhancement the information in these areas should become more visible for analysis. The density of the angiogram ranges from approximately .05 to 1.05 as will be demonstrated by the input histogram.

To simplify matters, only digital contrast enhancement is to be exercised; hence, the analog contrast constant, E_A, of Equation (32) must equal one for E_D equal one or from Equation (20) $D_{max} - D_{min} = d_{max} - d_{min}$. Assuming that the entire density range of the print film is exploited by the display, then $d_{max} = 1.6$ and $d_{min} = 0.02$ which is a density difference of 1.58. In order to satisfy the requirement that E_A equals one, the analog input parameters were adjusted using the Kodak Density Step Wedge, to include the needed density difference of 1.58.

In the first scan no digital contrast enhancement, $E_D = 1.0$, was used; therefore, the output print should theoretically resemble the transparency in contrast since E_A also equals one. The resulting output picture is shown in Figure 37 which does appear to closely exemplify the input contrast. Also an input histogram and a computer wedge are exposed on this print and all those that follow in the section from which the input and output density ranges may be checked. The input histogram shows that there is no saturation at either end of the range; therefore, all the information exists in the density range of 1.58 which was mentioned above.

Quite often a very gentle slope, $E_D \ll 1.0$, is employed in the regions where no input densities occur thus preserving the output density range for the regions where the input densities prevail. The second scan expands the input density over the entire output density range of the film with the contrast enhancement slopes shown in Figure 38 together

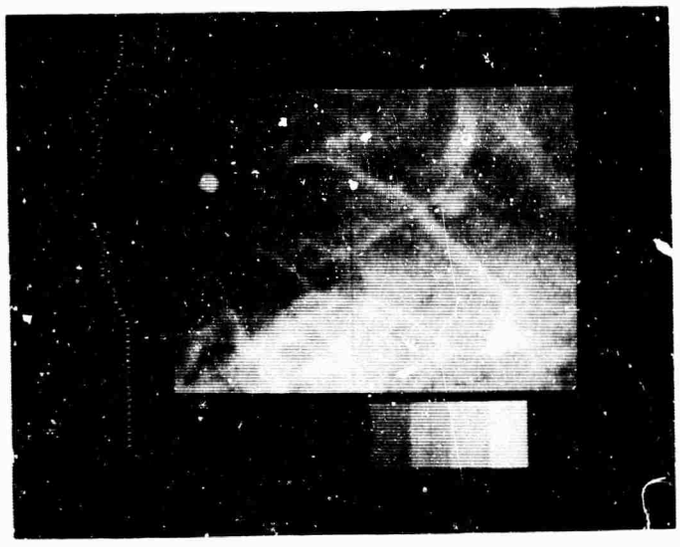

(a) Displayed Picture

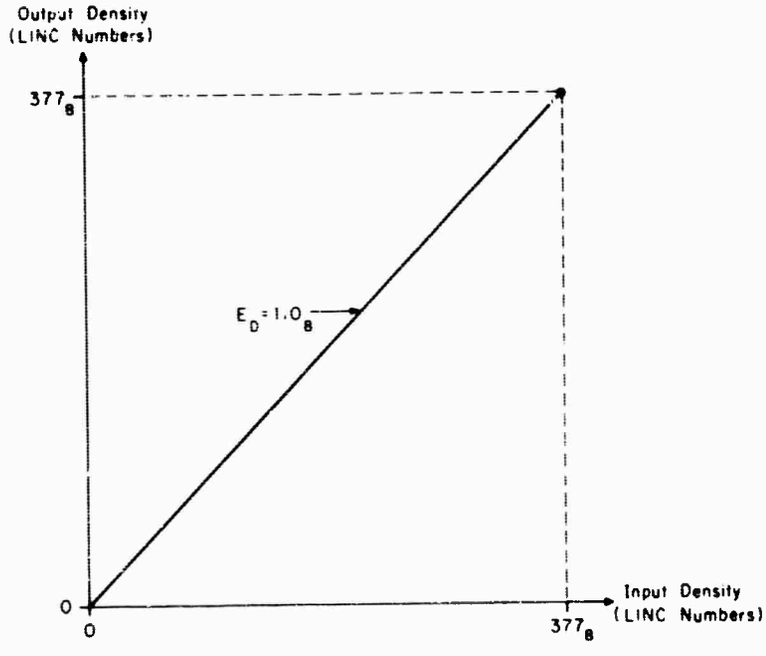

(b) Contrast Enhancement Function

Figure 37. Results of Unity Contrast Enhancement

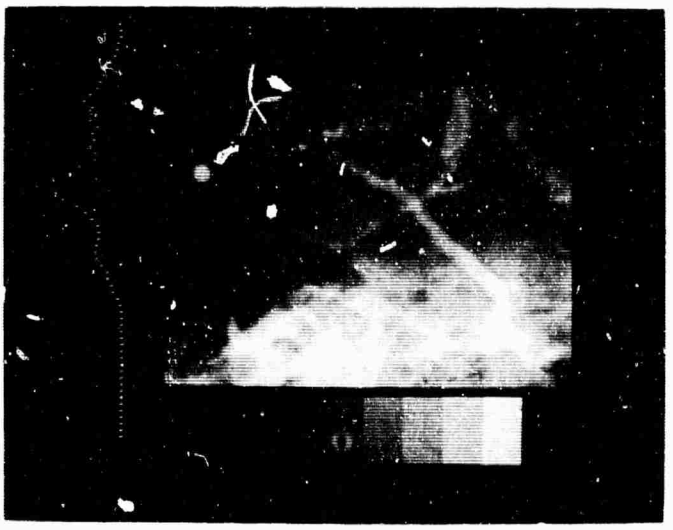

(a) Displayed Picture

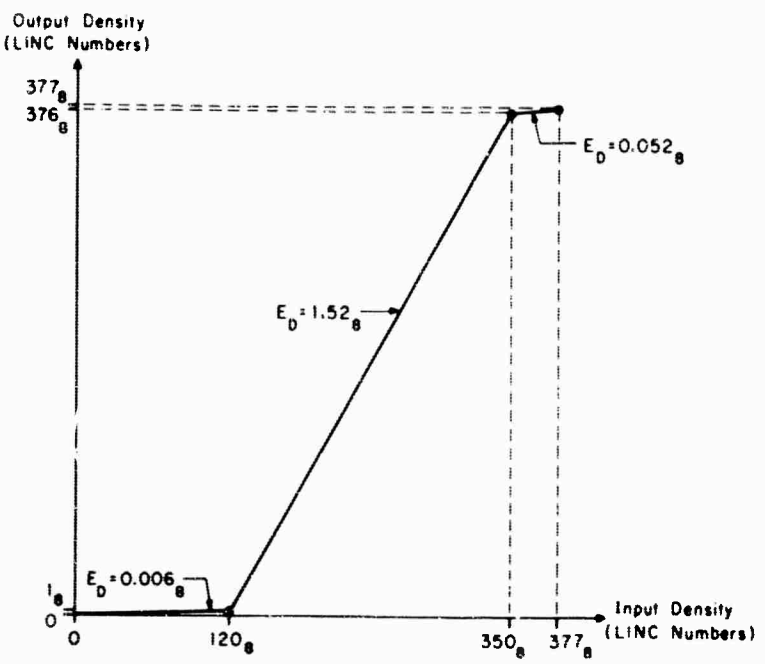

(b) Contrast Enhancement Function

Figure 38. Contrast Enhancement Using Film's Complete Density Range

with the resulting picture. Here the contrast enhancement is evenly distributed throughout the transparency's densities without emphasizing any particular region. Comparing the pictures of Figure 37 and 38 shows that in the latter, more contrast has been attained and consequently more visible information.

For the next scan, the contrast enhancement slopes are roughly proportional to the amplitude of the peaks of the input histogram. Such a procedure implies that the frequently occurring input densities are enhanced more than the sparsely occurring input densities thereby increasing the contrast where most of the information exists. However, the slopes are selected such that none of the data is compressed as shown by the slopes in Figure 39 along with the resulting print. In performing this type of contrast enhancement as much detail as possible is retained and at the same time the contrast is increased in a select section.

For the picture of Figure 40, the slopes were adjusted to enhance only the higher density areas in the original picture, while the data in the lower densities approached film saturation and in some places the detail has been completely washed out. But the information in the higher densities is more easily resolved than in any of the previously presented pictures. This can be especially noted in the left hand region of the print where the contrast of the finger-like vessels has been augmented. The reverse, increasing the contrast in the lower densities, is shown in Figure 41. As the slopes indicate, the detail contained in the low input contrast areas is suppressed even further into the film background. Most of the smaller vessels in the lower densities have now become better defined in Figure 41 because of the

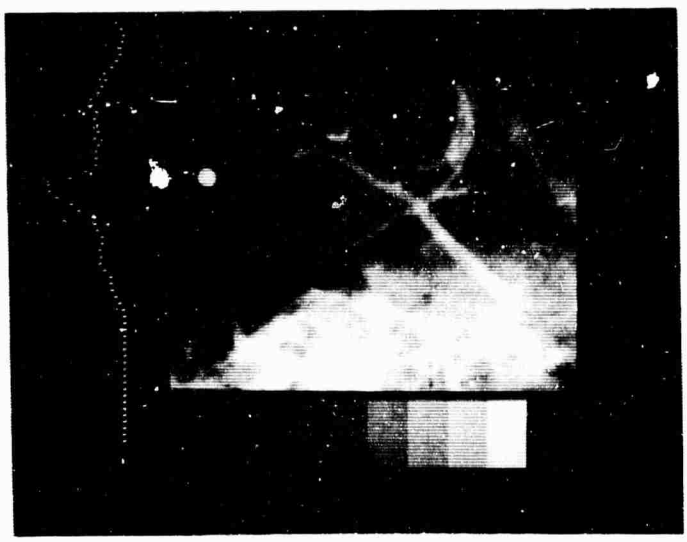

(a) Displayed Picture

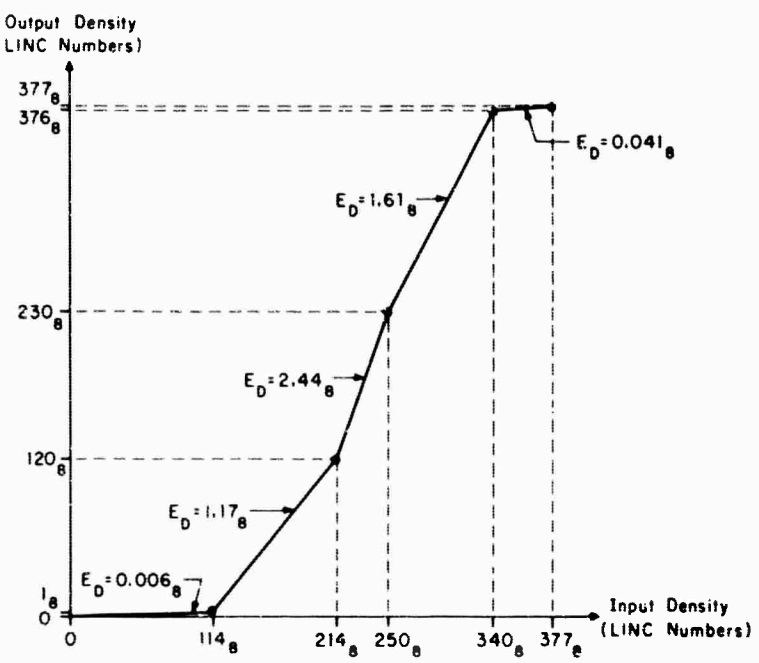

(b) Contrast Enhancement Function

Figure 39. Contrast Enhancement Proportional to Histogram's Population

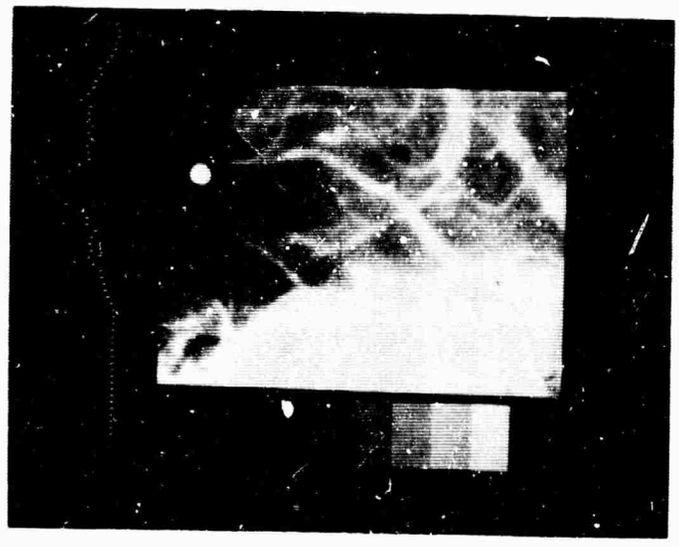

(a) Displayed Picture

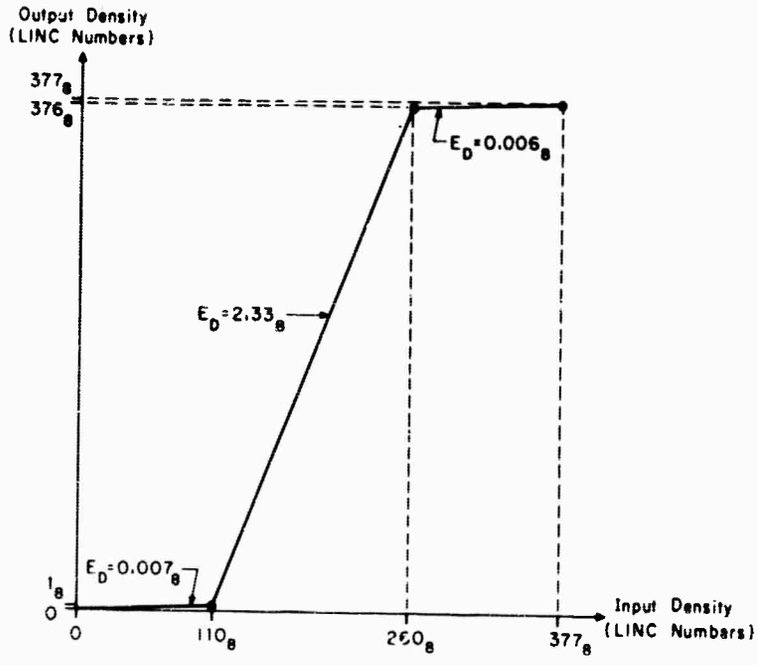

(b) Contrast Enhancement Function

Figure 40. Contrast Enhancement in High Density Areas

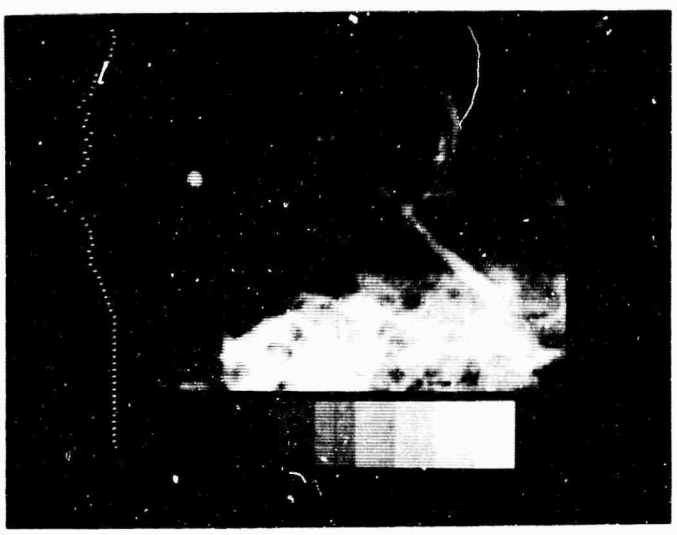

(a) Displayed Picture

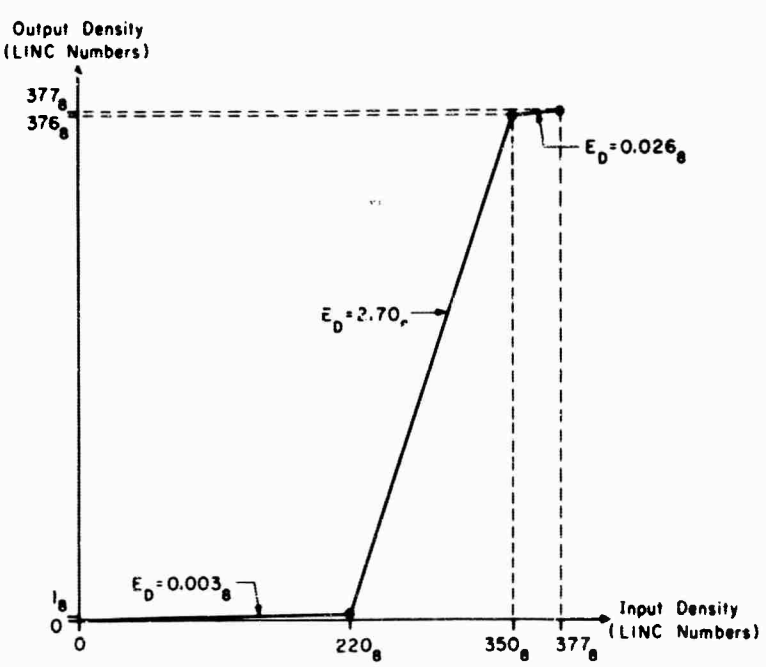

(b) Contrast Enhancement Function

Figure 41. Contrast Enhancement in Low Density Areas

increase in contrast. The bright area at the bottom of the picture also manifests more information than in Figure 37. Ideally, one would desire the latter picture's enhancement without sacrificing the information in the higher densities since significant data prevails in the lower densities.

With the above sequence of pictures the contrast enhancement program has proven itself to be very instrumental in assisting in the analysis of low contrast transparencies. These pictures were procured by attempting several different slopes with input histogram providing some guideline in selecting these slopes until satisfactory output results were attained. Ideally, the derived equations should lead directly to the slopes that yield the desired output contrast once such contrast has been defined.

5. THE SUBTRACTION TECHNIQUE

In radiology the problem of analyzing a sequence of time related films frequently occurs and angiograms, which primarily consider the blood vessels, have received much attention. The first radiograph of the angiographic series is exposed under normal conditions and is referred to as the base-line film of the sequence. Immediately afterwards a contrast medium is injected into the blood vessels of the immobilized patient and then subsequent radiographs are exposed in a relatively short span of time. The injected dye flowing through the blood vessels increases the contrast of the angiogram. From the series, the radiologist endeavors to subtract the base-line film from each of the others by conventional viewing and thereby derive the difference information. This type of analysis entails a vast amount of experience and even then, some information is not detected because of low contrast and because of the difficulty of mental subtraction. However, to increase the contrast on the angiograms implies that the dosage of contrast material must be augmented beyond a safe level. Therefore, other techniques have been developed to improve the detection of difference detail by means of subtracting two angiograms and manifesting the resulting information in picture form. Three completely different subtaction techniques which will be briefly described are the following: (1) photographic; (2) video; and (3) color subtraction methods.

5.1 SOME METHODS THAT HAVE BEEN RESEARCHED

The photographic procedure involves converting one of the two angiograms to a negative image or diapositive which is then superimposed precisely on the other roentgenogram. From these two a composite picture

is photographically procured. Theoretically, only uncommon information should appear on the composite image but in practice misalignment and an imperfect densitometric diapositive reduce the quality of the subtracted picture. To improve the subtraction the exposure, development and registration are varied in a time consuming trial and error procedure. To date, the photographic method has met with limited success and is seldom employed primarily because of the critical adjustment required and the time element involved (23, 24).

Several video subtraction techniques are presently available and are discussed in some detail in the literature. One particular and rather successful method employs two identically designed television cameras of the vidicon type except with opposite polarity such that one of the cameras displays a diapositive image, (23). The cameras are equipped with electronic controls for focus, gain, contrast, brightness, and linearity. Each of the angiograms is scanned by one of the cameras which are properly synchronized. The output images of the cameras are superimposed on a single monitor thereby displaying a subtracted image. With the subtracted image as a reference, the two radiographs are positioned with respect to each other until the optimum alignment appears. The primary disadvantage of this video subtraction stems from the fact that perfectly matched television cameras are unobtainable. Therefore, much time is expended in adjusting the electronic controls of both cameras although the amount of time is far less than with the photographic method. One compensating factor is the capability of the television cameras to enhance the contrast and thus retrieve information in low contrast regions. This procedure has been of some practical assistance but further improvement in the electronic equipment is essential.

The color subtraction method is based on the principle of color addition which is simply the production of a third color light by the addition of the light of two primary colors (24). Fundamentally, two light sources with variable light intensity control are positioned at right angles to each other. Both sources are covered with opal glass and a beam-splitting mirror is inserted at a 45 degree angle between the light sources. Different color filters are placed over each light source and a radiograph over each filter. Again the subtracted image is referred to in aligning the angiograms and for adjusting the intensity of each light source. Cancellation occurs as a result of common information transmitting equal amounts of filtered light. The composite image is then recorded on Polaroid black and white film from which an analysis is readily performed. The advantages of this technique over the photographic and video methods are reliability, simplicity, and low cost. However, several different color filters must be applied in an attempt to extract as much information as possible. Furthermore, the contrast of the subtracted picture cannot be enhanced.

5.2 DESCRIPTION OF THE PRESENT SYSTEM

Because of the limited success of these and other processes to perform subtraction between two serial radiographs, the image processing system's characteristics were investigated. The attractive features of the system are the image dissector camera's freedom to scan in any desired pattern and its contrast enhancement capability. In addition, the same camera scans both radiographs; thus there is no need to maintain an exact balance between cameras as is required in the two camera video subtraction technique. In order to examine these two advantages a computer program was designed to perpetrate subtraction on two

transparencies. The procedure of the subtraction program is explained in the remainder of the section.

The radiographs to be subtracted were positioned on the surface of the light source and then scanned. However, the problem of aligning the two roentgenograms with respect to each other had to be solved. In the initial stages the radiographs were aligned on a "light table" and marked with small registration rectangles cut into the radiographs. With one rectangle on each radiograph, only the horizontal and vertical displacements, and not the rotational error in alignment, were to be controlled by the computer. If the rotational alighment were to be controlled, a second rectangle would have to be placed on the radiographs. This formed the prototype by which the two input transparencies to be subtracted could be accurately aligned. Such registration rectangles could easily be created in practice by inserting small rectangular pieces of lead into the field of view when exposing the sequence of radiographs.

Figure 42 delineates the arrangement of the two roentgenograms for subtraction purposes. Rotational error is minimized by aligning and then carefully attaching the two pictures together; therefore, any rotation in one would be compensated for in the other. The horizontal and vertical alignment procedure is outlined in the schematic of Figure 42, where the dotted lines represent a continuous scan and solid lines represent a jump from one point to the other. This method was implemented into a computer program which basically detected the edges of the registration rectangles. The flow chart of Figure 43 describes the

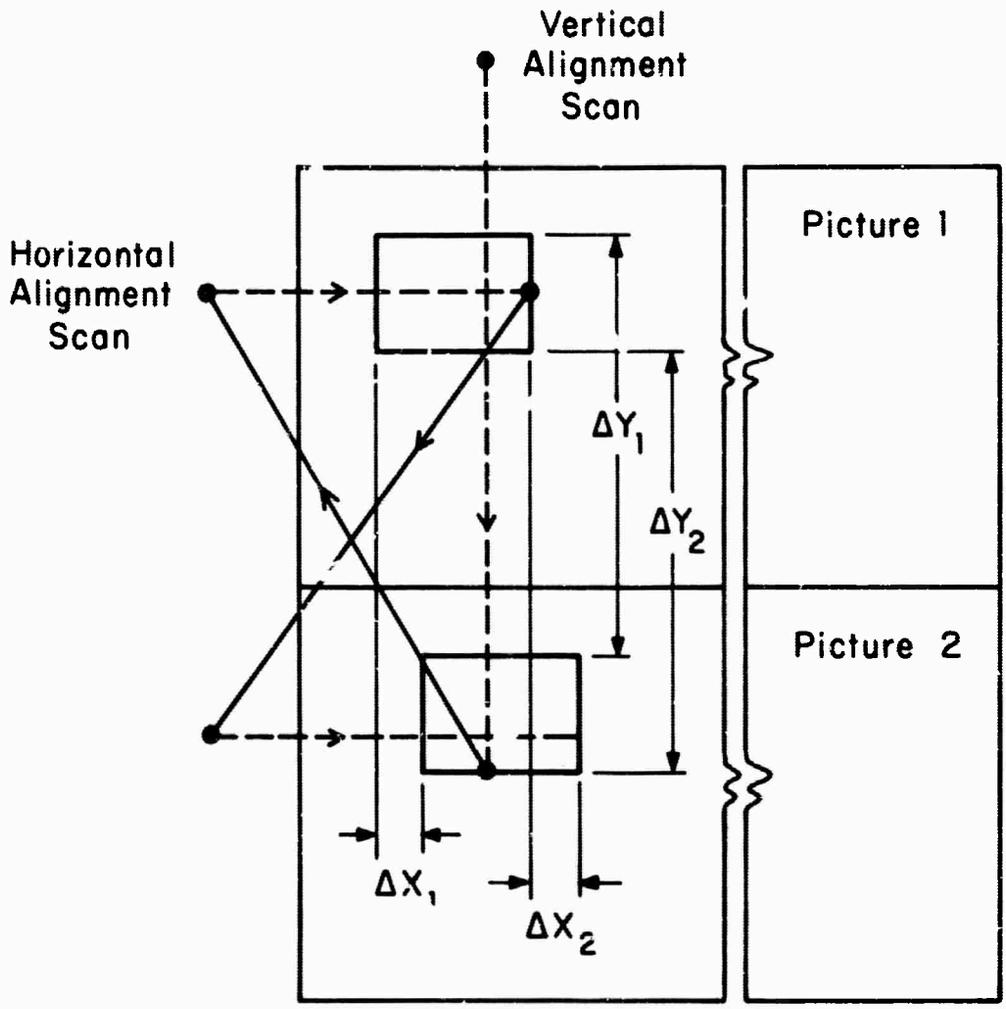

Figure 42. Schematic Illustrating Alignment Procedure

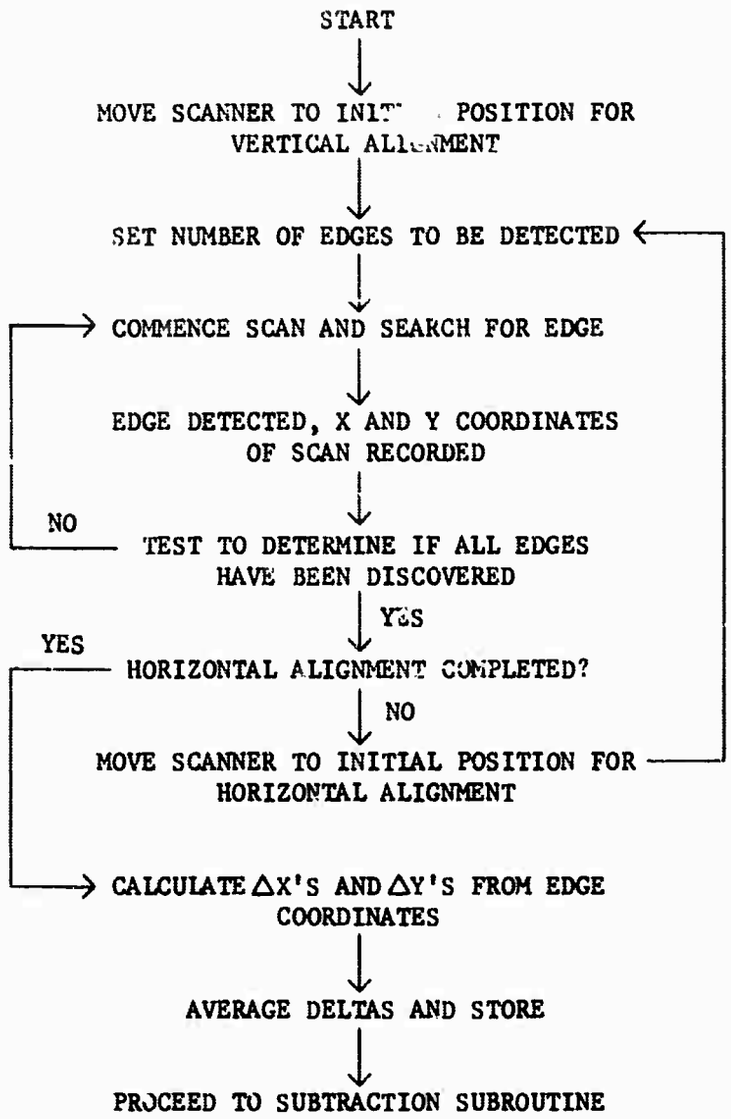

Figure 43. Flow Diagram of Vertical and Horizontal Alignment Subroutine

operations of the alignment subroutine. As Figure 42 illustrates, all four edges of each rectangle were discovered; and from the coordinates, the alignment adjustments are calculated by direct averaging.

After the vertical and horizontal corrections have been ascertained, video subtraction may be executed according to the flow diagram of Figure 44. The procedure commences by scanning and recording in memory a horizontal line of picture one. Next, the scanner is positioned, by means of the registration factors, to scan the identical line of picture two. Theoretically, each point in the line of transparency two corresponds directly to a point of picture one. Therefore, while scanning the second picture, each input point is subtracted from its counterpart in the other picture by referring to memory. The absolute density difference between the two radiographs defines the information for the subtracted image. For each subtraction a point is displayed with an intensity related to the density difference by modulating the z-axis of the oscilloscope accordingly. Thus the output density decreases as the input density difference increases. Upon completing the scan of the line in picture two, the next horizontal line of picture one is scanned and recorded and the entire process continued until both radiographs have been completely scanned or commanded to terminate. The subtracted image is, by time exposure, as usual, photographed on Polaroid film for immediate evaluation.

The contrast enhancement subroutine was easily modified to a form that was incorporated into the subtraction program. In this situation the contrast enhancement slopes process the absolute density differences between the angiograms. By enhancing the contrast of small density differences which results from low contrast radiographs, increased

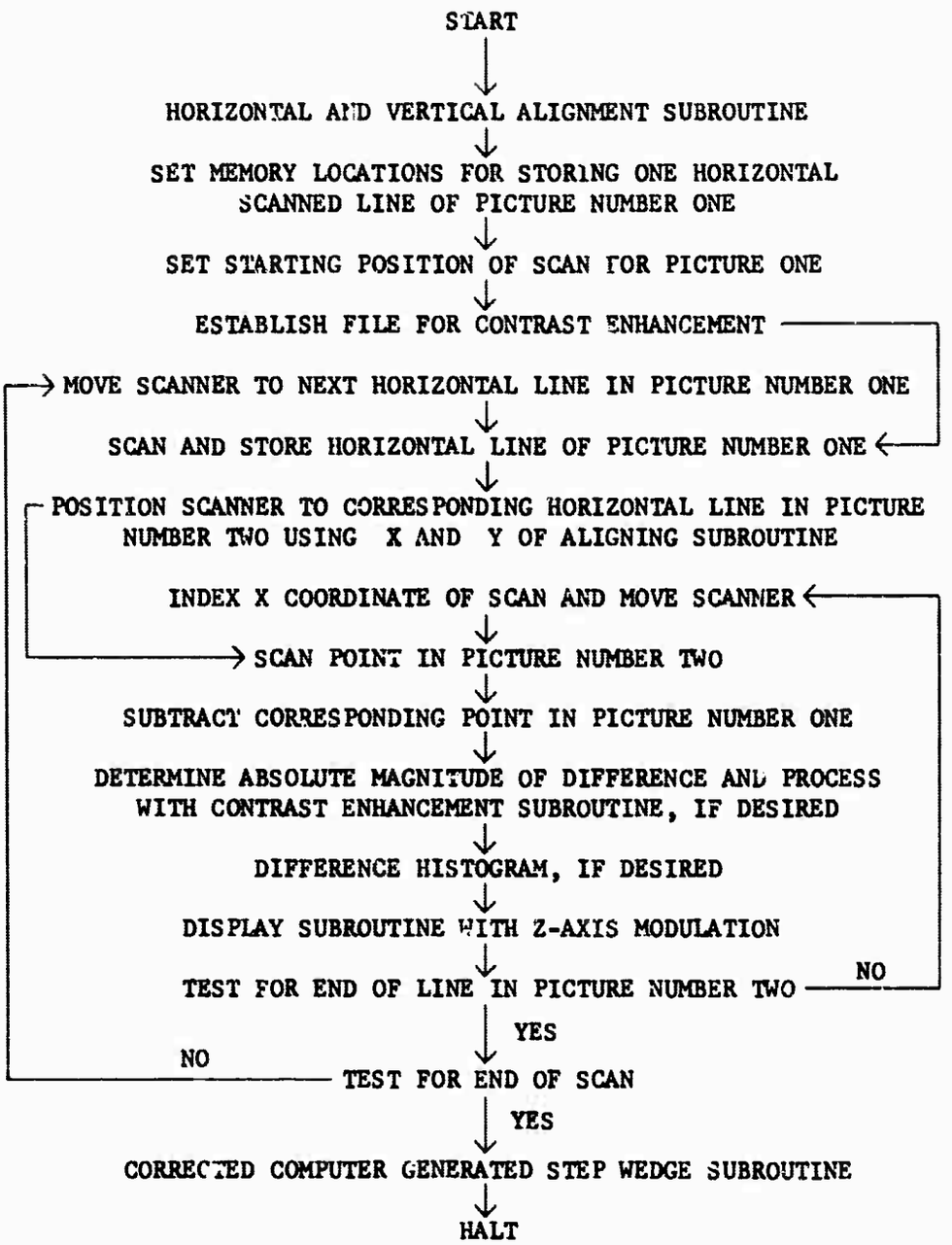

Figure 44. Flow Chart for Subtraction Program

awareness of information in areas of poor contrast is brought about. The histogram subroutine is also available to assist in the setting of contrast enhancement slopes; however, the density differences rather than the input densities are represented by the histogram.

5.3 RESULTS

The two angiograms which were subtracted were also individually scanned, processed and displayed with the final results shown in Figure 45. The subtracted image with contrast enhancement is presented in Figure 46 together with the digital slopes. The subtracted picture manifests the uncommon information which consists primarily of the blood vessels with the injected opaque dye. Most of the bony structure, the bright area at the bottom of the radiographs, cancelled and is suppressed into the background of the subtracted image. However, some detail does exist in the region, for example the fork-like vessel indicated in Figure 42. The circular object common to both inputs has been successfully subtracted thereby demonstrating that the digital alignment procedure functioned properly and that no significant rotational displacement occurred.

By deliberately offsetting the alignment, the print of Figure 47 was produced. Here the subtracted image is degraded because the common information is not completely subtracted. The vertical structure in the lower left hand corner of the picture appears as a consequence of the misalignment.

The subtraction technique is not restricted to angiograms but can be applied to any field where time related pictures are analyzed for differences. For example, military aerial photographs of terrain are

Figure 45. Input Angiograms for Subtraction

(a) Displayed Picture

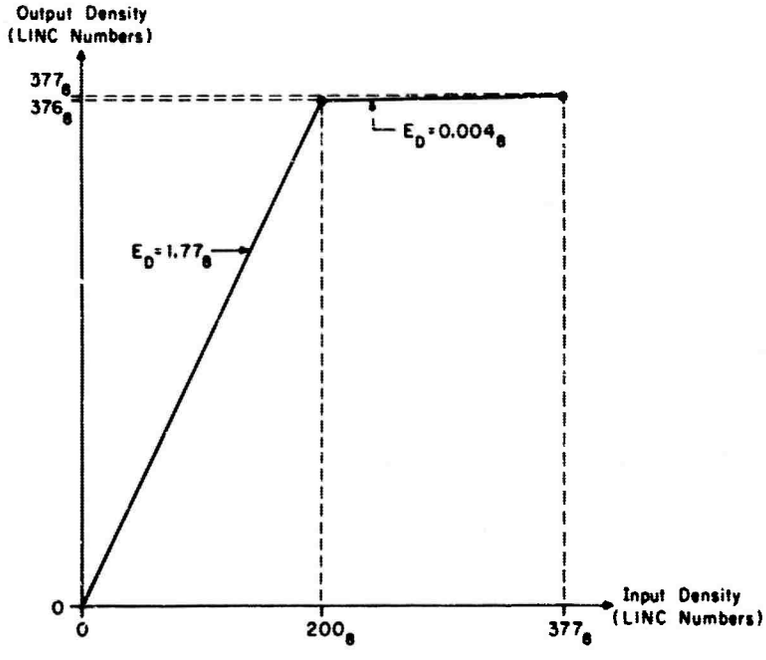

(b) Contrast Enhancement Function

Figure 46. Subtracted Image

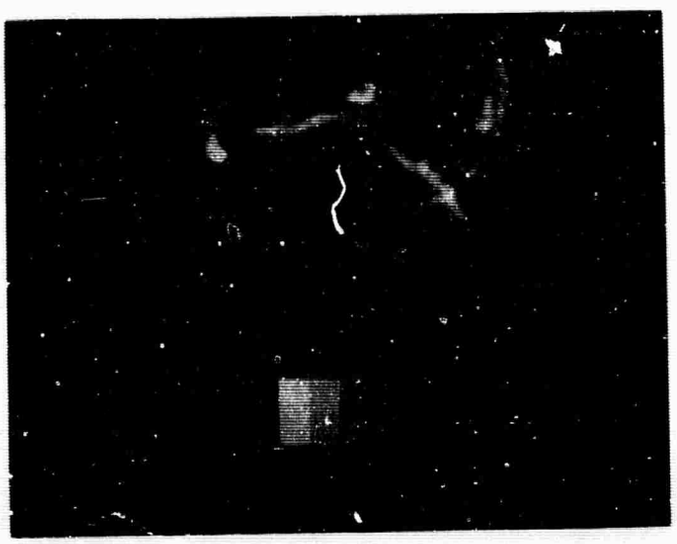

Figure 47. Subtracted Image Showing Misalignment

inspected for discrepancies which might disclose enemy movement. Moreover, the pictures from space explorations might be examined for differences to determine if any life exists. As for the field of medicine, the subtracted image between two time related pictures could assist in surmising if a condition has improved, remained steadfast or become worse.

6. SUMMARY AND CONCLUSION

This research has successfully demonstrated the feasibility of an on-line image processing system using the image dissector camera and a computer with a small core memory. The hardware and software which have been developed can provide the basic tools for the solution of a variety of image processing problems. In addition, the system should be useful as a preprocessor for a multilevel gray optical pattern recognition system.

Although several types of scanning devices are available, the image dissector camera has one of the best performance to cost ratios. The two most attractive features of the image dissector camera besides the low cost are its linear density spectrum and random scan capability. Higher quality devices have been devised, namely electronic flying-spot scanners; however, the cost multiplies proportionately. Furthermore, most current flying-spot scanners are designed to scan only 35 or 70 millimeter film thereby requiring some photographic or optical processing on larger images before scanning. The image dissector camera's input field is easily adjusted to almost any reasonable size. The storage type television cameras are difficult to program scan while micro-densitometers are normally slow because of the mechanical motion.

It has been the philosophy of this research to try to achieve an optimum balance between those functions performed by analog circuitry and those performed in the digital computer. The analog circuitry has a definite advantage in establishing the proper offset and gain so that full use can be made of the plus or minus one volt input range of the digital computer. When it is desired to work with the signals that are

proportional to density, which requires the logarithm of the camera's voltage, an analog operation is much more efficient than doing the operation in the computer where the quantization of the input signal would be a limitation. Moreover, the analog circuitry can be made much faster than the corresponding operation in the digital computer, and since more than 131,072 points are processed in each picture, this can be a great benefit. However, the digital computer has the capability of being able to mechanize much more complicated processes and it is easy to change these processes in very accurate manners.

From the research it was concluded that the display apparatus of the present system has the following limitations: (1) maximum size of 500 by 500 point display field whereas the scanner is capable of 1000 by 1000; (2) nonuniform brightness over the tube face; (3) the film density versus cathode voltage is nonlinear; (4) film graininess and uneven development; and (5) the scope's intensity drifts slightly with time. On the other hand, the density range is sufficient to exploit the film's density span. Also, the fast development film enables the system to operate on-line, thus sacrificing some quality for speed. The nonuniformity of the display is avoided simply by restricting the output images to the most uniform area. Finally, the output display nonlinearity was easily overcome by means of a digital correction program.

The digital contrast enhancement program is capable of regulating the contrast in specific density regions of the input. The program is easily adjustable such that the contrast can be enhanced or compressed in any region. As the quantitative results exhibited, information in poor contrast areas is extracted for viewing by enhancing the contrast.

The results also indicate that increasing the contrast in one density region frequently decreases the contrast in another section.

The derived equations representing the image processing system's operations are important since the factors controlling the degree of enhancement can be more rigidly determined. The equations have been verified with experimental data to be within plus or minus ten percent which is a maximum error. Although this is a significant discrepancy, it appears that almost all of the error can be attributed to uneven development of the film and other experimental problems rather than to the theory presented. Even though the equations predict the output contrast, the minimum contrast required between two objects for detection involves several psychological factors which have not as of yet been completely understood. The system's equations also show that the contrast cannot be increased without bounds but eventually reaches a saturation point due to film limitations.

Although the contrast enhancement procedure is effective, the magnitude of the improvement in picture information is not as much as was anticipated. Some of the reasons for this are the film saturation, the restricted resolution of the present system, information limitations in the input pictures themselves, and other effects mentioned above.

The alignment procedure of the subtraction program, although somewhat crude, does properly align two input angiograms with respect to each other as the results verify. Besides the obvious differences, the subtracted image presented in this report also manifests some difference information that is difficult for a radiologist to detect, especially in the cluttered bone area. The two important advantages of this subtraction technique over the video and color subtraction

methods are: (1) subtraction performed with one camera, and (2) the contrast of the subtracted image can be enhanced. If it were desired to do production runs with this routine, then a quicker, more convenient procedure which automatically takes rotational corrections into account could be considered.

The following are some of the directions that future research with the present equipment could take. One process that could be investigated is described by Selzer (4) whereby a digital filter modifies the frequency spectrum of a radiograph. The loss of information in a radiograph can be caused by any of several factors: (1) random distribution of roentgen quanta; (2) nonzero width of x-ray source causes a high frequency loss; (3) diffusion; (4) film graininess; (5) radiation scatter; and (6) bounceback in intensifying screens. Selzer employs a two dimensional filter that is the reciprocal of the modulation transfer of the roentgen system, and from his results this appears t accentuate the information of the radiograph.

Another setup which is presently being considered is the processing of microscopic images. Here the dissector camera views the image directly through the microscope's optical system thus an intermediate picture is not required. If the information is three dimensional, ideally then some processing could be executed and from the results the focus of the microscope modified in an attempt to follow an outline, such as would occur in exploring a neural network.

7. BIBLIOGRAPHY

1. Prince, M. D., "Man-Computer Graphics for Computer-Aided Design", Proceedings of the Institute of Electrical and Electronics Engineers, Vol. 54, No. 12, (1698-1708), December 1966.

2. "Purdue Conference on Instrumentation for High Energy Physics", IEEE Transactions on Nuclear Science, Vol. NS-12, No. 4, August 1965.

3. Nathan, R., "Digital Video-Data Handling", Jet Propulsion Laboratory Technical Report, No. 32-877, January 5, 1966.

4. Selzer, R. H., "Digital Computer Processing of X-Ray Photographs", Jet Propulsion Laboratory Technical Report, No. 32-1028, November 15, 1966.

5. Morgan, R. H., "The Frequency Response Function", The American Journal of Roentgenology, Radiation Therapy and Nuclear Medicine, Vol. 88, No. 1, (175-186), July 1962.

6. Morgan, R. H., Bates, L.M., Gopalarao, U.V., and Mavinaro, A., "The Frequency Response Characteristics of X-Ray Films and Screens", The American Journal of Roentgenology, Radiation Therapy and Nuclear Medicine, Vol. 92, (426-440), August 1964.

7. Fink, D.G., Principles of Television Engineering, McGraw-Hill Book Company, Inc., New York, (63-165), 1940.

8. Brown, C.J., "Resolution of Flying-Spot Scanner Systems", Institute of Electrical and Electronics Engineers Spectrum, Vol. 4, No. 8, (73-78), August 1967.

9. Nielsen, R.S., and Ford, M.A., "DiScan: Versatile Image Sensor", Optical and Electro-Optical Information Processing, Tippett, J.T., Berkowitz, D.A., Clapp, L.C., Koester, C.J., and Vanderburgh, Jr., A., The Massachusetts Institute of Technology Press, Massachusetts, 1965.

10. Hobbs, L.C., "Display Applications and Technology", Proceedings of the Institute of Electrical and Electronics Engineers, Vol. 54, No. 12, (1870-1884), December 1966.

11. Van Dam, A., "Computer Driven Displays and Their Use in Man/Machine Interaction", Advances in Computers, Alt, F.L., and Rubinoff, M., Academic Press, New York, Vol. 7, 1966.

BIBLIOGRAPHY
(continued)

12. Kazmierczak, H., and Steinbuck, K., "Adaptive Systems in Pattern Recognition", Institute of Electrical and Electronics Engineers Transactions on Electronic Computers", Vol. EC-13, No. 6, December 1963.

13. Schreiber, W. F., "Picture Coding", Proceedings of the Institute of the Electrical and Electronics Engineers, Vol. 55, No. 3, (320-330) March 1967.

14. Graham, L. N., "Image Transmission by Two-Dimensional Contour Coding", Proceedings of the Institute of Electrical and Electronics Enginners, Vol. 55, No. 3, (336-346), March 1967.

15. Holmes, W. S., "Automatic Photointerpretation and Target Location", Proceedings of the Institute of Electrical and Electronics Engineers, Vol. 54, No. 12, (1679-1686), December 1966.

16. Solomonoff, R. M., "Some Recent Work in Artificial Intelligence", Proceedings of the Institute of Electrical and Electronics Engineers, Vol. 54, No. 12, (1687-1697), December 1966.

17. Minsky, M. L., "Artificial Intelligence", Scientific American, Vol. 216, No. 3, (246-260), September 1966.

18. Ledley, R. S., Rotolo, L. S., Golab, T. J., Jacobson, J. D., Ginsberg, M. D., and Wilson, J. B., "FIDAC: Film Input to Digital Automatic Computer and Associated Syntax-Directed Pattern-Recognition Programming System", Optical and Electro-Optical Information Processing, Tippett, J. T., Berkowitz, D. A., Clapp, L. C., Koester, C. J., and Vanderburgh, Jr., A., The Massachusetts Institute of Technology Press, Massachusetts, 1965.

19. Harris, J. L., Sr., "Image Evaluation and Restoration", Journal of the Optical Society of America, Vol. 56, No. 5, (569-574), May 1966.

20. Clark, W. A., and Molnar, C. E., "A Description of the LINC", Computers in Biomedical Research, Vol. II, edited by Stacy, R. W. and Waxman, B., Academic Press, New York, N.Y., (35-04) 1965.

21. Wilkes, M.A., and Clark, W. A., "Programming the LINC", Computer Research Laboratory, Washington University, St. Louis, Missouri, June 1965.

22. "Spectral Response and Sensitometric Data for Polaroid Land Black and White Film", Polaroid Technical Information, Bulletin F34423D, October 1966.

23. Hanafee, W., and Stout, P., "Subtraction Technic", Radiology, Vol. 79, No. 4, (658-661), October 1962.

24. Wise, R. E., and Ganson, J., "Subtraction Technic: Video and Color Methods", Radiology, Vol. 86, (814-821), May 1966.

Unclassified
Security Classification

DOCUMENT CONTROL DATA - R & D

(Security classification of title, body of abstract and indexing annotation must be entered when the overall report is classified)

1. ORIGINATING ACTIVITY *(Corporate author)*
Computer Systems Laboratory
Washington University,
724 South Euclid, St. Louis, Missouri 63110

2a. REPORT SECURITY CLASSIFICATION
Unclassified

2b. GROUP

3. REPORT TITLE

Development of an On-line Image Processing System for the LINC

4. DESCRIPTIVE NOTES *(Type of report and inclusive dates)*
Interim-Technical

5. AUTHOR(S) *(First name, middle initial, last name)*

John E. Guignon, Jr. and Raymond M. Kline

6. REPORT DATE	7a. TOTAL NO. OF PAGES	7b. NO. OF REFS
February, 1968	121	24

8a. CONTRACT OR GRANT NO.
(1) DOD (ARPA) Contract No. SD-302
(2) NIH (DRFR) Grant No. FR-00218

b. PROJECT NO.
(1) ARPA Project Code No. 5880
c. Order No. 655
d.

9a. ORIGINATOR'S REPORT NUMBER(S)
Technical Report No. 5

9b. OTHER REPORT NO(S) *(Any other numbers that may be assigned this report)*

10. DISTRIBUTION STATEMENT

Distribution of this document is unlimited

11. SUPPLEMENTARY NOTES

12. SPONSORING MILITARY ACTIVITY
ARPA-Information Processing Techniques
NIH-Div. of Research Facilities

13. ABSTRACT

The development of an on-line image processing system for the LINC computer is described with both hardware and software details being considered. The purpose of the system is to operate on various types of optical images endeavoring to process them so that a maximum amount of useful information is retrieved for final interpretation by the observer. Besides other processing techniques, contrast enhancement and subtraction have been implemented into the system to achieve this purpose. A mathematical model of the system is investigated and equations describing its capabilities are derived. Results showing several pictures before and after processing as well as data verifying the mathematical model are also presented.

DD FORM 1 NOV 65 1473 REPLACES DD FORM 1473, 1 JAN 64, WHICH IS OBSOLETE FOR ARMY USE.

Security Classification

14. KEY WORDS	LINK A		LINK B		LINK C	
	ROLE	WT	ROLE	WT	ROLE	WT
LINC Interfacing						
Image Dissector Camera						
Analog Preprocessing Circuitry						
Display equipment						
Scan Program						
Display Methods						
Dot Matrix Technique						
Intensity Modulation Procedure						
Enhancement Process						
Analysis of Simple Linear System						
Analysis of Experimental System						
Subtraction Technique						
Contrast Enhancement as means of Reclaiming Picture Information						